



2023

## Effect of Selenof Loss in Combination with a Western Diet on Tumorigenesis

Brenna Joy Flowers

Follow this and additional works at: [https://ecommons.luc.edu/luc\\_theses](https://ecommons.luc.edu/luc_theses)

 Part of the [Oncology Commons](#)

---

### Recommended Citation

Flowers, Brenna Joy, "Effect of Selenof Loss in Combination with a Western Diet on Tumorigenesis" (2023). *Master's Theses*. 4473.

[https://ecommons.luc.edu/luc\\_theses/4473](https://ecommons.luc.edu/luc_theses/4473)

This Thesis is brought to you for free and open access by the Theses and Dissertations at Loyola eCommons. It has been accepted for inclusion in Master's Theses by an authorized administrator of Loyola eCommons. For more information, please contact [ecommons@luc.edu](mailto:ecommons@luc.edu).



This work is licensed under a [Creative Commons Attribution-NonCommercial-No Derivative Works 3.0 License](#).  
Copyright © 2023 Brenna Joy Flowers

LOYOLA UNIVERSITY CHICAGO

EFFECT OF SELENOF LOSS IN COMBINATION WITH A WESTERN DIET ON  
TUMORIGENESIS

A THESIS SUBMITTED TO  
THE FACULTY OF THE GRADUATE SCHOOL  
IN CANDIDACY FOR THE DEGREE OF  
MASTER OF SCIENCE

PROGRAM IN CELLULAR AND MOLECULAR ONCOLOGY

BY

BRENNA FLOWERS

CHICAGO, IL

AUGUST 2023



## ACKNOWLEDGEMENTS

This project would not have been possible without the guidance and teaching of my mentor, Dr. Kastrati. I cannot thank her enough for welcoming me into her lab and giving me so many opportunities to further my education. I would also like to thank my committee for their invaluable guidance and for taking the time to teach me.

I owe a special thanks to Alexandra Zigrossi for teaching me an incredible amount over the past two years and for her invaluable help and support throughout this project.

Thank you to my friends and family for providing much-needed encouragement and levity throughout this journey, no matter how far away. Finally, but certainly not least, I would like to thank my partner, Jarrett Collins, for his unwavering support (whether in Chicago or Los Angeles) and for always believing in me.

## TABLE OF CONTENTS

ACKNOWLEDGEMENTS .....	iii
LIST OF FIGURES .....	v
LIST OF TABLES .....	vi
ABSTRACT .....	vii
CHAPTER I – INTRODUCTION.....	1
Breast Cancer Background .....	1
Selenium, Selenoproteins, and Their Role in Breast Cancer .....	2
SELENOF, Its Role in Breast Cancer, and Related Functions .....	5
Hypothesis.....	8
Specific Aims .....	14
CHAPTER II – RESULTS.....	16
Selenof Levels in Mice .....	16
Mouse Weights.....	20
Fasting Glucose Measurements .....	21
Overall Tumor Burden .....	23
Tumor Incidence .....	30
Mammary Tumorigenesis .....	30
CHAPTER III – DISCUSSION.....	32
Conclusion .....	35
CHAPTER IV – MATERIALS AND METHODS.....	36
Selenof Knockout Mice .....	36
Mouse Housing and Diets .....	36
DMBA Preparation and Protocol.....	37
Weight, Lesion, and Glucose Measurements .....	37
Sample Preparation and Analysis.....	38
Genotyping.....	38
Western Blot.....	39
RT-Quantitative PCR (QPCR) .....	40
3D Acinar Assay .....	40
Statistical Analysis .....	41
REFERENCE LIST .....	42

## LIST OF FIGURES

Figure 1. Summary of the Proposed Functions of SELENOF from Flowers et al 2023 .....	7
Figure 2. Loss of SELENOF in MCF-10A Cells Results in Increased Proliferation .....	10
Figure 3. Loss of SELENOF in MCF-10A Cells Results in Abrogated Cell Death .....	12
Figure 4. Schematic of Study Design and End-Points .....	13
Figure 5. Selenof Expression Levels in Mammary Glands of Representative Mice .....	17
Figure 6. Genotyping Results of WT Mice .....	18
Figure 7. Genotyping Results of Selenof KO Mice .....	19
Figure 8. Average Body Weights of WT ND, WT WD, Selenof KO ND, and SELENOF KO WD Cohorts .....	21
Figure 9. Average Fasting Glucose Measurements of Mice .....	22
Figure 10. Increased Tumor Multiplicity in Selenof KO Mice is Largely Due to Skin Tumors ..	25
Figure 11. Representative H&E Slide of a Mammary Tumor .....	26
Figure 12. Representative H&E Slide of a Thymus Lymphocytic Lymphoma .....	27
Figure 13. Representative H&E Slides of Sebaceous-Squamous Cell Carcinomas .....	28
Figure 14. Representative H&E Slides of Squamous Cell Carcinomas .....	29
Figure 15. Tumor Incidence is Increased in Selenof KO Mice .....	31

LIST OF TABLES

Table 1. Number of Mice with Tumors at End-Point Stratified by Organ..... 24

Table 2. Number of Tumors in Each Cohort at End-Point Stratified by Organ..... 24

Table 3. Thermal Cycler Protocol for Genotyping ..... 39

## ABSTRACT

SELENOF is an understudied selenium-containing protein that has previously been postulated to behave as a tumor suppressor in the breast. Examination of patient databases showed that SELENOF levels were lowest in tumors from patients with aggressive late-stage breast cancers. Whether loss of SELENOF drives breast tumorigenesis remains to be determined. To address this question, we used juvenile female wild type or systemic Selenof knockout mice and exposed them to 7,12-Dimethylbenz[a]anthracene (DMBA), a carcinogen that replicates the multistep process of breast tumorigenesis. Previous reports have shown that loss of Selenof led to glucose and metabolic dysregulation in mice suggesting a link between Selenof and metabolism. Because obesity is a risk factor in breast cancer, we challenged the mice with a Western diet, high in fats and calories, to mimic obesity. We hypothesized that loss of Selenof would promote DMBA-induced tumorigenesis and the Western diet would exacerbate it.

We found that overall tumor incidence was in fact highest in the Selenof knockout mice and Western diet group. However, mammary tumor incidence was equal between the Selenof knockout and wild type cohorts. The Selenof knockout mice did not exhibit higher weights, however, they did exhibit higher fasting glucose levels, consistent with metabolic dysfunction. These findings indicate that the link between SELENOF, obesity, and breast cancer warrants further investigation.



## CHAPTER I

### INTRODUCTION

#### **Breast Cancer Background**

Breast cancer is the most diagnosed cancer in U.S. women, accounting for 30% of new cancer diagnoses and the second leading cause of cancer-related death in the United States [1]. The disease is mainly classified into three subtypes based on the presences of estrogen receptors (ER), progesterone receptors (PR), and human epidermal growth factor receptor 2 (HER2) [2, 3]. If ER and/or PR are present, the disease is classified as hormone receptor positive (HR+) and endocrine therapy is available for treatments [3]. Overexpression of HER2 classifies the disease as HER2+, for which anti-HER2 therapeutics are available [3]. If there is no overexpression of HER2 or ER/PR, it is classified as triple negative breast cancer (TNBC), for which chemotherapy is the main therapeutic option and a limited number of patients benefit from PARP inhibitors or immunotherapy [3]. Unfortunately for all three subtypes, recurrence and resistance to current treatment options are common [2]. While the 5-year survival rate is 99.3% for localized disease, even with current therapeutic options, the 5-year survival rate for distant (metastatic) disease is only 31% (<https://seer.cancer.gov/statfacts/html/breast.html>). Due to the above-mentioned rise of resistance, recurrence, and lack of better targeted therapies, research into new targets and treatments for breast cancer is needed in addition to a deeper understanding of breast cancer biology.

## **Selenium, Selenoproteins and Their Role in Breast Cancer**

Selenium (Se) is an essential trace element consumed in food, especially those high in Se such as chicken, fish, and Brazil nuts (Selenium – Fact Sheet for Health Professionals <https://ods.od.nih.gov/factsheets/Selenium-HealthProfessional/>) [4, 5]. There is a U-shaped curve relating Se levels and health risk, meaning when too little or too much Se is present, adverse health effects arise, with the optimal Se level identified to be approximately 125 ug/L [2, 4, 5]. Inappropriately low Se levels have been implicated in many diseases that are otherwise preventable with Se supplementation, such as Keshan disease (a type of cardiomyopathy) and Kashin-Beck disease (a type of osteochondropathy) [2, 5]. Additionally, low Se levels have been shown to hamper immune function, which can lead to an increased risk of cancer [2].

Based on the benefits of adequate Se and the negative consequences of low Se, the role of Se as a chemopreventative agent in cancer has been explored [2, 6]. Interest in using Se as a nutritional supplement for cancer prevention dates back to the 1970s and was sparked by reports of an inverse association between Se status and the risk for multiple types of cancer, including breast cancer [7]. Se supplementation as a chemopreventative agent in prostate cancer yielded unfavorable results. In general, Se supplementation above adequate levels of Se has not shown therapeutic or chemopreventative benefits in breast cancer [2, 8]. Instead, newer data has shown that when compared to inadequate levels of Se, higher levels of Se correlate with better patient outcomes in breast cancer but have no effect on breast cancer incidence [2, 9-15]. Many of these studies were conducted in geographical areas with suboptimal Se levels in soil, such as Europe and China, and therefore may not be applicable to areas such as the United States (U.S), where the Se levels are generally replete [2, 16, 17].

One large study investigating the connection between Se and breast cancer conducted within the U.S. is the Women's Healthy Eating and Living (WHEL) study, which did not show correlation between Se dietary intake and breast cancer survival [2, 18, 19]. This is expected as participants resided in the U.S. Their intake was above the recommended daily intake of 55ug of Se per day, and as mentioned above Se above replete levels does not confer additional benefits [2, 4, 5]. A direct measure other than Se dietary intake would be beneficial since Se in the soil varies among different geographical areas. One option is toenail Se levels which are a more accurate measure of long-term Se status [17]. In fact, when toenail Se was used, variations in Se levels were noted in the U.S. population according to location, gender, ethnicity, alcohol and smoking habits, and level of education [17]. This highlights a problem with the previously mentioned studies in the U.S. that examined Se levels and cancer incidence – they rely on Se dietary intake only as opposed to a more accurate measure of Se status [8-10, 19].

Conversely, a study by Demircan et al (2021), one of the largest to date studying Se and breast cancer, did not extrapolate patients Se intake, but instead used patients' *Selenium Status* [20]. A patient's *Selenium Status* was determined by measuring serum Se levels, selenoprotein P (SELENOP) levels, and GPX1 activity [20]. Using patients' *Selenium Status* instead of their Se intake, the group demonstrated that breast cancer patients whose serum Se levels, SELENOP levels, and GPX1 activity were in the lowest quintile (deemed *Triple Deficient*) had significantly lower overall survival compared to patients who had even one marker in the highest quintile [20]. Even when only serum Se is examined, Lubinski et al. (2018) demonstrated breast cancer patients with serum Se levels in the lowest quartile had a five-year survival rate of 78% while patients with serum Se levels in the highest quartile had a five-year survival rate of 94% [14]. Sandsveden et al. (2020), including 1,003 breast cancer patients from the Malmö Diet and

Cancer Study, also demonstrated that serum Se levels inversely correlated to breast cancer mortality [21]. Yet, these studies did not examine Se levels within the breast tissue or in breast tumors. A study by Charalabopoulos et al. using a small patient cohort demonstrated that Se levels within neoplastic breast tissue were four times higher than normal breast tissue [12]. One reason postulated for this is that Se antioxidant effects are necessary to overcome the oxidative stress of breast tumors [2, 12]. Therefore, it is still unclear how circulating levels differ from breast tissue bioavailability and how that relates to breast cancer.

To summarize, the above studies have demonstrated that higher Se levels correlate with lower breast cancer mortality, however, have no impact on incidence [2, 14, 20, 21]. The emerging paradigm is that Se confers its biological activity through selenoproteins, indicating that selenoproteins should now be investigated more closely in breast cancer [2, 16].

Se is incorporated into proteins by the amino acid selenocysteine (Sec), commonly referred to as the 21st amino acid [22]. Sec has its own tRNA, like the other 20 amino acids, and has the same backbone as cysteine (Cys), but with a Se in place of a Sulfur (S) conferring an increased redox potential [22, 23]. As Sec is encoded by UGA, which is usually a stop codon, the UGA is recoded for Sec with the assistance of the Selenocysteine Insertion (SECIS) element in the 3'-untranslated region (UTR) of Sec containing proteins (selenoproteins) [22, 24-26]. In eukaryotes, the elongation factor EFsec binds to the Sec tRNA (Sec-tRNA<sup>[Ser]Sec</sup>) and then binds to SECIS binding protein 2 (SBP2), which is bound to the SECIS element [25, 27]. Selenoproteins are highly conserved and occur in bacteria, eukaryotes, and archaea [25]. There are 25 selenoproteins encoded within the human genome [2]. Some have known functions, mainly as oxidoreductases in part due to the increased redox potential of Sec over Cys, while the function of others is still unclear [28].

The function of all selenoproteins in relation to breast cancer has been investigated using a mouse model with *Trsp* knocked out in the mammary glands only, resulting in the loss of the Sec tRNA, and therefore the loss of all selenoproteins [29]. The authors found that their *Trsp* knockout model had increased breast cancer incidence and shorter survival than the wild type (WT) mice [29], indicating that selenoproteins are involved in mammary gland carcinogenesis [2, 29]. How each selenoprotein contributes to breast cancer is largely unknown.

### **SELENOF, Its Role in Breast Cancer, and Related Functions**

Selenoprotein F or SELENOF (formerly Sep15) is a 15kDa selenoprotein residing on chromosome 1 at locus 31 [30-32]. In a study done using a Chicago cohort of samples from cancer patients, loss of heterozygosity of SELENOF was seen in breast tumors [2]. SELENOF is also highly responsive to Se bioavailability, indicating that it can mediate the beneficial actions of Se [17, 25, 26, 33, 34]. Yet, no studies examining a potential role for SELENOF were reported in breast cancer. SELENOF is located in the endoplasmic reticulum and bound to UDP-glucose:glycoprotein glucosyltransferase (UGGT) (Figure 1) [35]. The Sec of SELENOF resides in a thioredoxin-like fold, indicating it may be active in disulfide bond formation in protein folding and redox quality control [35]. In 2022, Zigrossi et al. reported that SELENOF is a new tumor suppressor in breast cancer [6]. In this study, the overexpression of SELENOF in MCF-7 (HR+ breast cancer cells) attenuated proliferation, increased cell death and response to standard-of-care therapeutics, and elicited anti-tumor activity in a xenograft model[6]. SELENOF expression was lowest in late stage tumors (stage III and IV) from breast cancer patients and lower expression predicted poor patient outcomes [6]. Based on these premises, investigating how the loss of SELENOF drives breast tumorigenesis is warranted.

Recent literature suggests that SELENOF may play a role in lipogenesis and glucose metabolism as well, however these studies are observational and descriptive, therefore lacking molecular mechanisms (Figure 1) [35-37]. The loss of Selenof in male C57Bl/6 mice resulted in increased weight gain, blood glucose levels, and poorer performance on glucose and insulin tolerance test when the Selenof knockout (KO) mice were fed a high-fat diet compared to wild type mice [36]. Additionally, Selenof KO mice had altered expression levels in proteins relating to fatty acid synthesis, while ATP and NADPH levels varied significantly in the liver cells [36]. This indicates that a loss of Selenof in a murine model affects the metabolism of mice exposed to high-fat diets [36]. This is consistent in a model using yellow catfish, where an excess intake of Se caused an increase in SELENOF expression levels and glycogenolysis through the SELENOF-dependent AKT1-FOXO3a-PYGL axis as well as an increase in triacylglycerides and glucose, also in a SELENOF-dependent manner [37]. Together these data indicate that SELENOF may have a possible role in glucose metabolism and lipogenesis. Please refer to the diagram in Figure 1 for a summary of known and putative functions of SELENOF (also reviewed in [2, 38]).

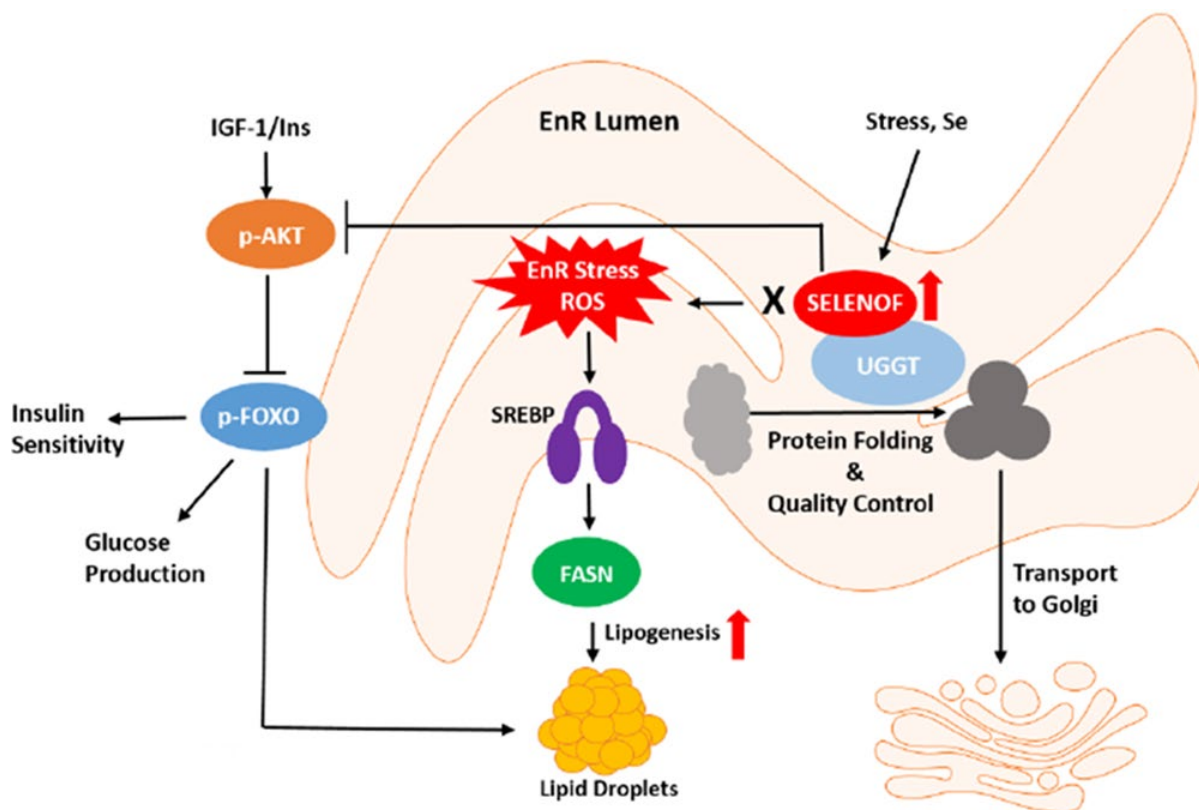


**Figure 1. Summary of the Proposed Functions of SELENOF from Flowers et al 2023.**

SELENOF is responsive to Se bioavailability, with an increase in Se corresponding to an increase in SELENOF expression. Data has implicated the role of SELENOF includes protein folding and quality control because it is a thioredoxin-like protein associated with UDP-glucose:glycoprotein glucosyltransferase in the endoplasmic reticulum. Recent studies have also suggested that the loss of SELENOF leads to increased lipogenesis and dysregulated insulin sensitivity and glucose production. However, these studies are observational and descriptive and lack a clear molecular mechanism. The proposed functions are reviewed in [38].

The loss of SELENOF, resulting in metabolic dysfunction and obesity, is of interest in breast cancer because obesity is an independent risk-factor of breast cancer in post-menopausal women [18, 39, 40]. It is thought that obesity increases the exposure to estrogens [39, 40] in part due to the storage of estrogen and precursors in adipose tissue, as estrogen levels have been observed to be higher in some obese post-menopausal women as well as the aromatization of

androstendione and testosterone to estrogen [39, 40]. Other likely contributors include: IGF, inflammation, cytokines, microbiota etc.

To determine how the loss of SELENOF affects breast tumorigenesis, the well-accepted model of 7,12-Dimethylbenz[a]anthracene (DMBA)-induced chemical carcinogenesis was used. DMBA is a polycyclic aromatic hydrocarbon [41]. This compound is a carcinogen that has historically been used in Sprague-Dawley (SD) rats to study mammary tumorigenesis [41, 42]. DMBA is metabolized by the cytochrome P450 enzymes CYP1A1 and CYP1B1 to produce reactive intermediates that form DNA adducts [43] which are repaired through nucleotide excision [44]. Nucleotide excision repair can be error-prone and introduce mutations [43, 44]. The mammary tumorigenic effects of DMBA are most effective in mice when administered prior to 10 weeks of age, due to the proliferation of terminal end buds during mammary gland development – allowing the maximum amount of DNA damage to be incorporated into the mammary gland at this step of increased proliferation [42]. In SD rats, DMBA was less effective as a mammary carcinogen in ovariectomized rats, suggesting the need for ovarian hormones in DMBA induced mammary tumorigenesis [41]. Advantages of using DMBA to study mammary tumorigenesis is that it mimics the multi-step process of mammary tumors, and it interrogates the gene/protein of interest in an immune-intact mouse model [41, 42].

### **Hypothesis**

**Hypothesis:** The loss of Selenof combined with a Western diet will promote mammary tumorigenesis in mice.

This hypothesis is based on the compelling evidence that loss of SELENOF results in oncogenic cellular transformation (Ekyalongo et al, 2023, manuscript undergoing revisions). We



utilized the MCF-10A cells, a spontaneously immortalized but non-transformed human breast epithelial cell line [45] with high levels of SELENOF (Figure 2A). Stable CRISPR-Cas9 SELENOF knockout (KO) lines were derived from single-cell clones (Figure 2A). MCF-10A SELENOF  $+/+$  which had undergone mock selection (referred to as WT) or SELENOF KO clones were used as a well-established model to assess functional consequences from aberrations found in cancer [46]. We observed a significant increase in proliferation in a 2D culture over 6 days in SELENOF KOs compared to WT cells (Figure 2B). This increased proliferation was confirmed by increased EdU incorporation into the DNA and increased mRNA levels of the proliferation marker *MKI67* (Figure 2C-D). When MCF-10A cells are seeded in a matrix-rich 3D culture, acini-like spheroids form that are notable for the presence of a hollow lumen and recapitulate several aspects of mammary gland architecture *in vivo* [47, 48].

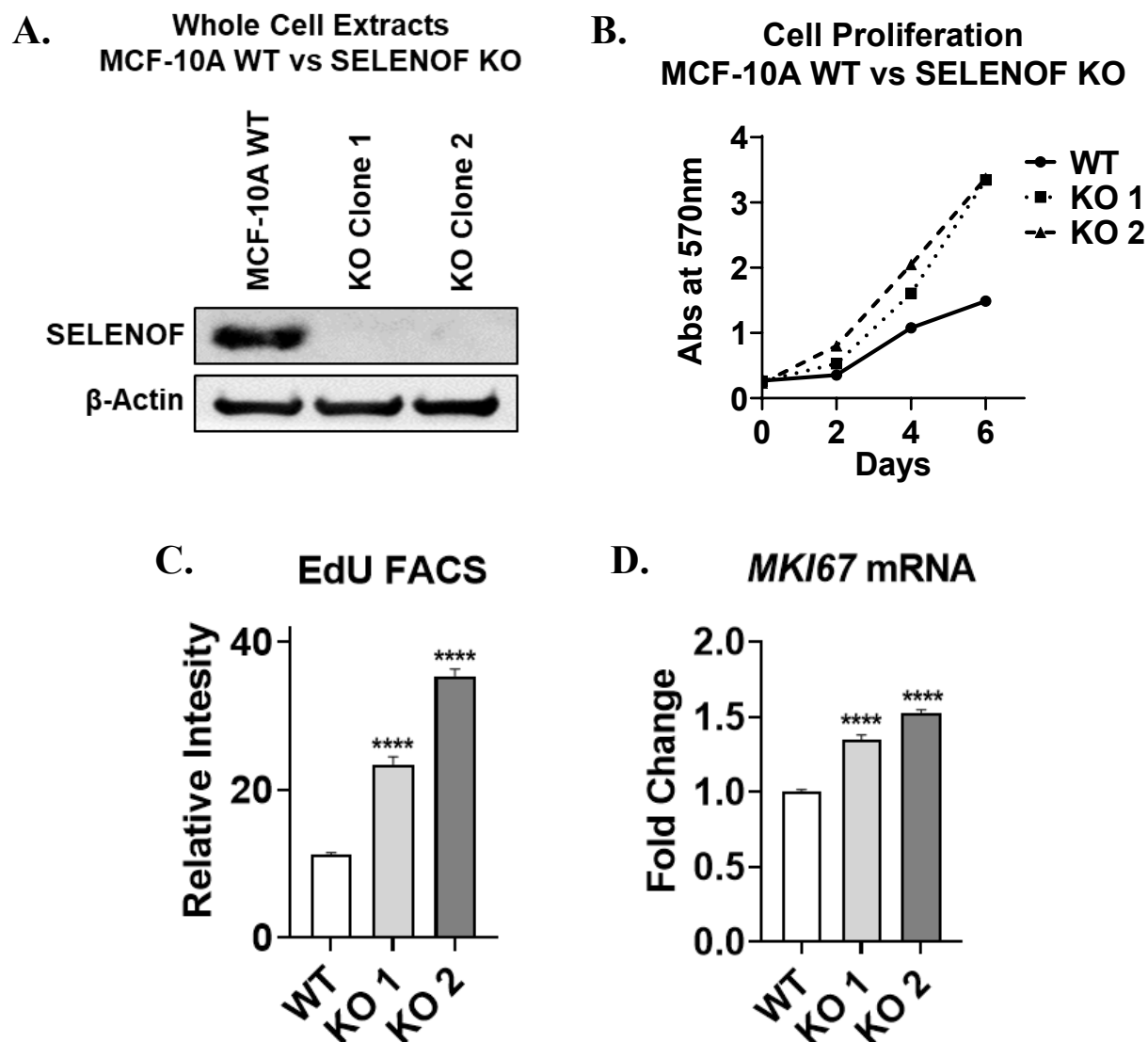


**Figure 2. Loss of SELENOF in MCF-10A Cells Results in Increased Proliferation.** A) SELENOF levels in MCF-10A sgRNA SELENOF +/+ Control (referred to as WT) and two representative SELENOF knockout (KO) clones (KO Clone 1 and KO Clone 2) shown in a western blot. The KO clones show no detectable SELENOF.  $\beta$ -actin used as a loading control. B) 2D growth of cells was determined by crystal violet. Absorbance at 570nm was measured over the course of 6 days. C) To confirm increased proliferation, the relative intensity of EdU incorporation into MCF-10A WT and SELENOF KO clones as determined by FACS. D) mRNA levels of the proliferation marker MKI67 was measured by RT-QPCR for MCF-10A WT and SELENOF KO clones. \*\*\*\* $p < 0.0001$

Deletion of SELENOF results in more and larger acini compared to WT controls (Figure 3). Seminal work by Dr. Brugge and colleagues demonstrated that while individual perturbation of cell proliferation or apoptosis pathways is insufficient to induce luminal filling, oncogenic dysregulation of both proliferation and apoptosis (e.g., by HER2) is sufficient to drive this process [49]. With caspase-mediated apoptosis, TRAIL-mediated autophagy results in lumen formation [50]. We find that loss of SELENOF in these cells results in luminal filling with live cells as demonstrated by Calcein AM staining of cells that fail to undergo cell death (Figure 3). Addition of apoptosis and autophagy inhibitors rescued cell death in WT, but had no effect in SELENOF KO acini (Figure 3, +ZVAD+CQ columns). While additional potential contributing mechanisms will be addressed in the future, abrogation of apoptosis and autophagy upon loss of SELENOF is precisely the opposite phenotype we observe with SELENOF overexpression [51].

**To summarize**, our data shows that loss of SELENOF increases cell proliferation and evasion of cell death, both hallmarks of oncogenic transformation [52]. Altogether, our data supports investigating whether the loss of SELENOF drives tumorigenesis *in vivo*.

## Fluorescence Imaging of 3D Acini

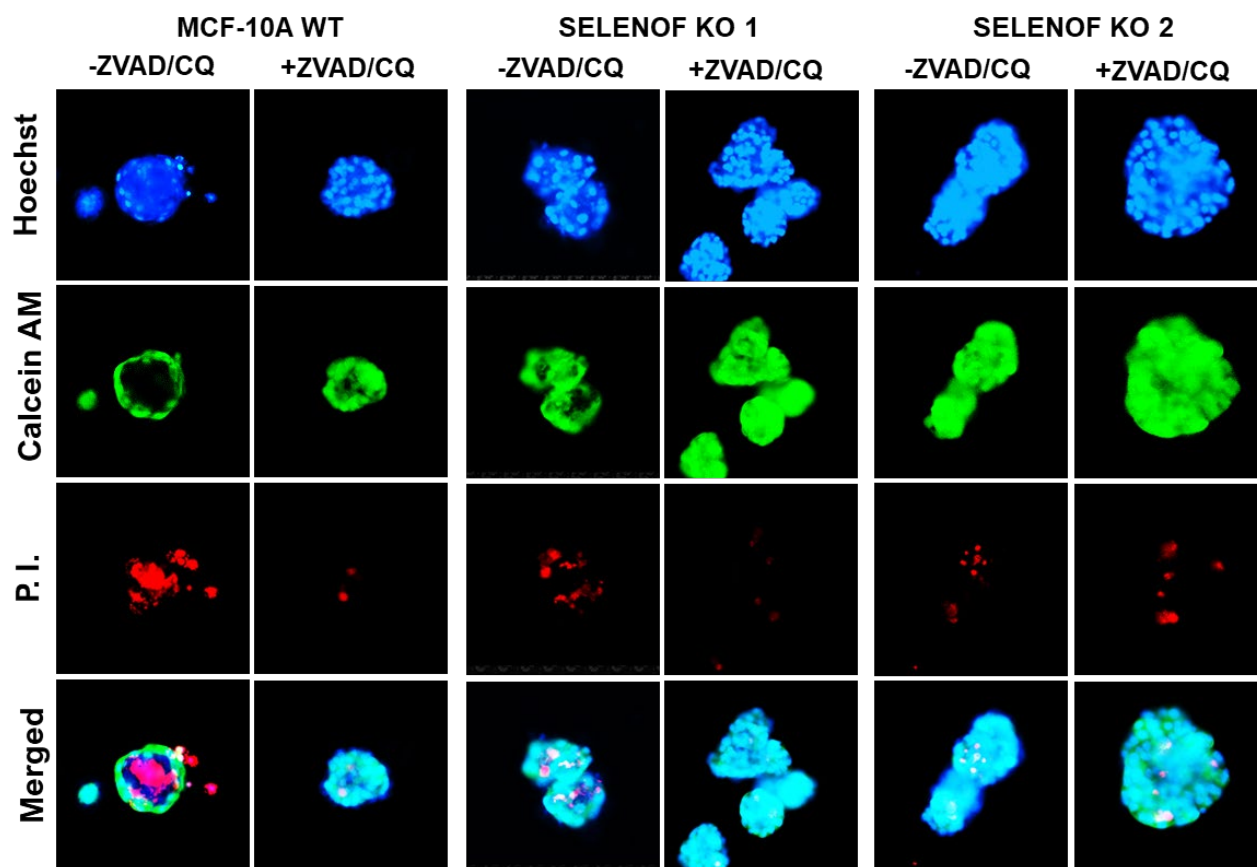


### Figure 3. Loss of SELENOF in MCF-10A Cells Results in Abrogated Cell Death.

Representative 3D acini grown in matrigel. Fluorescence imaging of live 3D acini grown in matrigel. Hoechst33342 (blue), Calcein AM (green) and propidium iodide (PI, red) indicate nuclear stain, live cells, or dead cells, respectively. ZVAD and chloroquine (CQ) were used to inhibit apoptosis and autophagy. In the SELENOF KO clones, live cells are present in the middle of the acini and there is decreased cell death in the middle. When ZVAD and CQ are added to the MCF-10A WT to inhibit apoptosis and autophagy, respectively, the same phenotype of increased live cells and decreased cell death in the middle occurs.

Obesity is a recognized risk factor for breast cancer [40]. Loss of Selenof together with high-fat diets exacerbated weight gain and the metabolic phenotype in mice [36, 37, 39, 40]. Taken together, we seek to elucidate how the loss of Selenof in a murine model combined with a high fat Western diet (WD) affects mammary tumorigenesis. To accomplish this, we will treat systemic Selenof KO and WT mice with 7,12-Dimethylbenz[a]anthracene (DMBA), and monitor for mammary tumors, recording tumor latency, size, and number. See diagram shown in Figure 4.

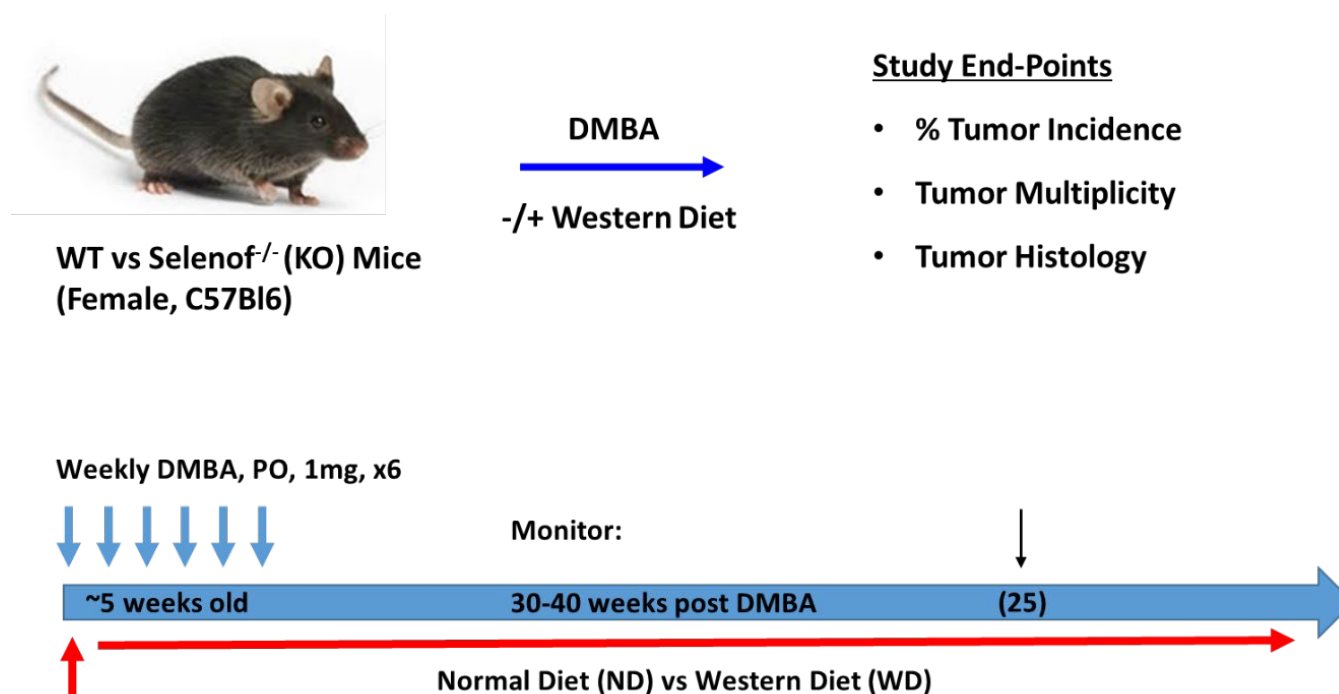


**Figure 4. Schematic of Study Design and End-Points.** Female Selenof KO and WT mice were randomized into a WD or ND cohort the same day DMBA exposure started. Each cohort (WT ND, WT WD, Selenof KO ND, and Selenof KO WD) consisted of 10 mice. The plan was to monitor mice for 30-40 weeks. However, due to many mice meeting end-point criteria earlier, the monitoring period was reduced to 25 weeks post DMBA exposure. Mice remained on the assigned diet for the entirety of the study. Study end-points were percents tumor incidence (how many mice presented with tumors), tumor multiplicity (how many tumors each mouse had), and tumor histology (tumor grade).

This will serve to determine if the loss of Selenof alone affects tumorigenesis. To determine if a WD contributes to breast cancer tumorigenesis and if the loss of Selenof exacerbates tumorigenesis when combined with the WD, we will randomize half of the WT and Selenof KO mice on WD chow. These mice will also be treated with a DMBA oral gavage once a week for six weeks, following the same protocol as those on normal chow. Weights will be taken weekly to monitor obesity criteria and fasting glucose readings will be taken prior to starting the WD and DMBA as well as periodically throughout the study period.

Our hypothesis will be addressed in the following aims:

### **Specific Aims**

Aim one: Determine if the loss of Selenof results in an increase in tumorigenesis *in vivo*.

Previous work by our lab has indicated SELENOF as a tumor suppressor *in vitro* in addition to previous research indicating the loss of all selenoproteins in mouse mammary glands increases mammary tumorigenesis [29]. However, how the systemic loss of Selenof specifically in a murine model affects mammary tumorigenesis has not been examined to our knowledge. In order to examine this, we will treat homozygous Selenof KO and WT mice with 7,12-Dimethylbenz[a]anthracene (DMBA), and monitor for mammary tumors, recording tumor latency, size, and number. This will serve to determine if the loss of Selenof affects tumorigenesis. I hypothesize that the loss of Selenof *in vivo* will increase DMBA-induced tumorigenesis.

Aim two: Determine whether consuming a WD in combination with loss of Selenof further increases mammary tumorigenesis.

It has previously been indicated that loss of Selenof renders male mice more susceptible to metabolic dysfunction and obesity [36]. Since obesity is a risk factor for breast cancer in postmenopausal women, we aim to examine if the loss of Selenof in combination with a WD increases mammary tumorigenesis.

We will place both WT and systemic Selenof KO mice on WD chow. The WT and Selenof KO mice in both the WD and normal chow cohorts will be treated with DMBA by oral gavage once a week for six weeks. Weights will be taken weekly to monitor obesity criteria and fasting glucose readings will be taken prior to starting the WD and DMBA as well as periodically throughout the study period. I hypothesize mice on the WD will have increased tumorigenesis and that the loss of Selenof will exacerbate this.

## CHAPTER II

### RESULTS

#### **Selenof Levels in Mice**

Selenof KO mice were previously derived by Kasaikina et al [53]. We verified Selenof loss by PCR genotyping, examining mRNA levels by RT-QPCR, and protein levels by western blot (WB). Since the Selenof KO mice had a portion of the *Selenof* gene replaced with a Neo cassette, the presence of a Neo cassette band was used as a positive control. Upon genotyping, wild-type (WT) mice had a band with for *Selenof* (Figure 6), while Selenof KO mice lacked a *Selenof* band, and a Neo cassette band was present (Figure 7). Selenof mRNA levels within the mammary glands of representative Selenof KO mice were undetectable after 40 cycles, while Selenof mRNA levels in the mammary glands of WT mice had an average cycle of 22.43 (Figure 5B).

DMBA is a stressor, and stress has been postulated to affect SELENOF levels [24, 35, 53]. In order to verify DMBA did not affect Selenof levels in WT or Selenof KO mice, a western blot for Selenof was performed on representative normal mammary gland samples. Normal mammary gland samples were taken from a Selenof KO mouse treated with DMBA, a Selenof KO mouse naïve to DMBA, a WT mouse treated with DMBA, and a WT mouse naïve to DMBA. Beta-actin was used as a loading control. All mice were age-matched. There was no Selenof expression in either mammary gland samples from the Selenof KO mice (Figure 5A). There was no significant difference in Selenof expression between the mammary glands of the



DMBA treated or naïve WT mice. The data thereby confirms that the Selenof KO mice used in this study lacked Selenof while the WT used had Selenof.

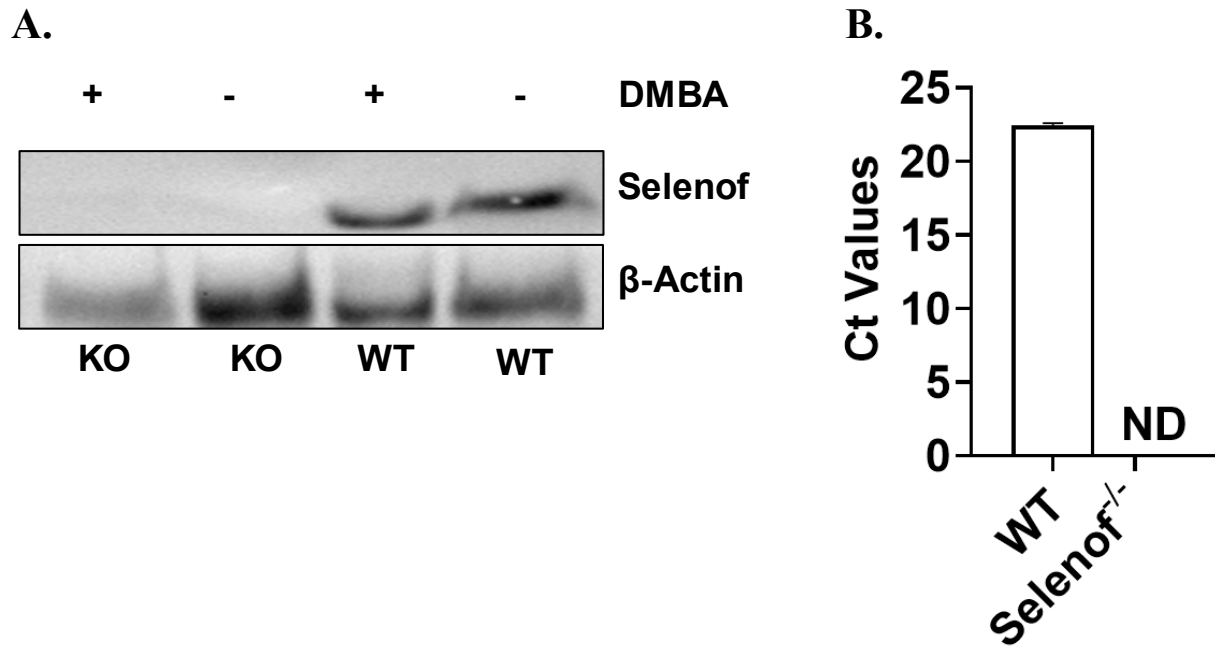


**Figure 5. Selenof Expression Levels in Mammary Glands of Representative Mice.** A) western blot of Selenof expression levels in whole tissue extracts of mammary glands of both DMBA treated and DMBA naïve Selenof KO and WT mice. Mice were age matched. B) *Selenof* mRNA expression in the mammary glands of WT and Selenof KO determined by RT-qPCR. *Selenof* was undetected after 40 cycles in Selenof KO mammary glands, therefore raw Ct values are shown.

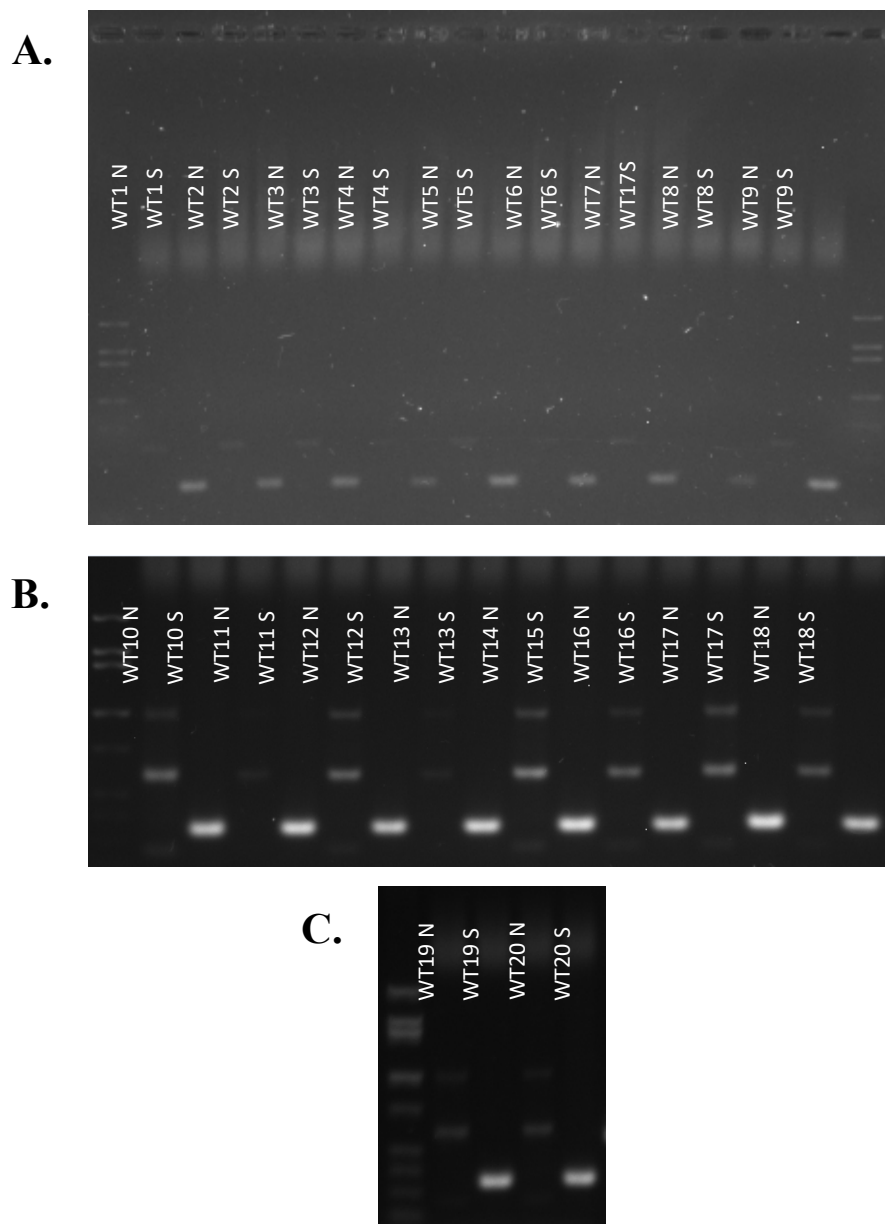
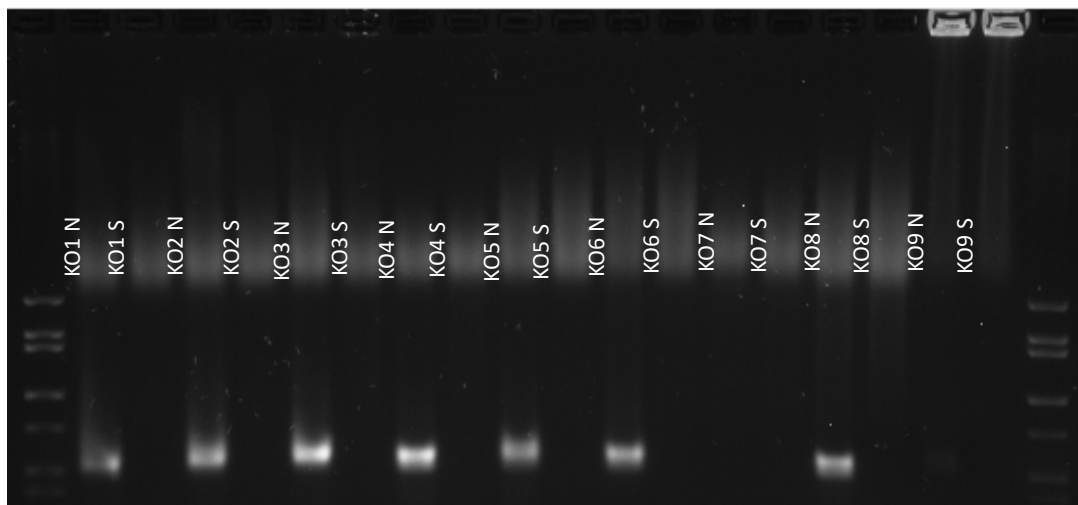
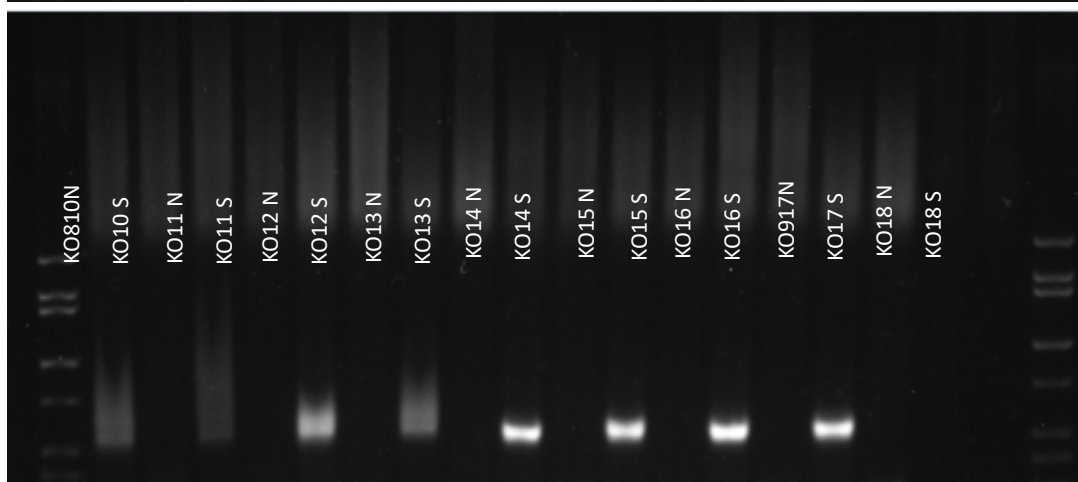


**Figure 6. Genotyping Results of WT Mice.** All mice in the study were genotyped to confirm Selenof status, using tail snips. “N” designates primers for the Neo cassette were used and “S” designates primers for Selenof were used. All WT mice showed a band for Selenof.

A.



B.



C.

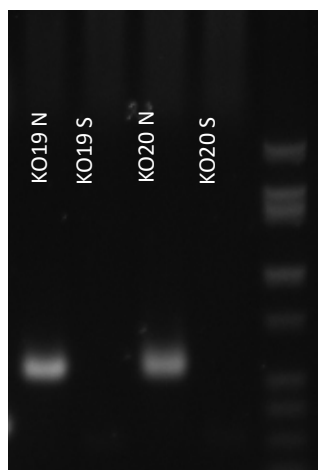


**Figure 7. Genotyping Results of Selenof KO Mice.** All mice in the study were genotyped to confirm Selenof status, using tail snips. "N" designates primers for the Neo cassette were used and "S" designates primers for Selenof were used. No Selenof KO mice showed a band for Selenof. Of note, DNA from KO9 was stuck in the wells and clean up attempts were unsuccessful.

### **Mouse Weights**

Mice were weighed weekly from the start of the protocol and through the entirety of the study. Weights were age-matched, averaged, and graphed for each cohort (Figure 8). A linear regression analysis determined that the slopes of WT ND, WT WD, Selenof KO ND, and Selenof KO WD were different enough that they would not intersect (Figure 8). Additionally, a two-way ANOVA determined the WT WD mice weighed significantly more than the WT ND and Selenof KO WD cohorts (Figure 8). The Selenof KO WD cohort weighed significantly more than the Selenof ND cohort (Figure 8). Interestingly, the Selenof KO WD did not have increased body weights compared to the WT ND group (Figure 8). This data indicates that the loss of Selenof alone does not result in increased weight gain, even when mice were challenged with a WD.

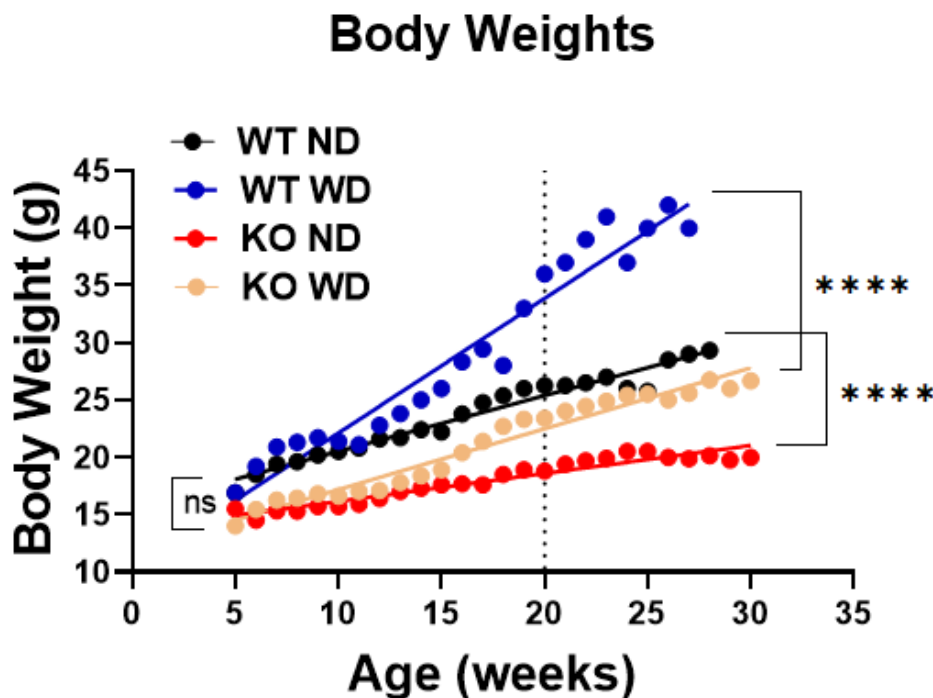


**Figure 8. Average Body Weights of WT ND, WT WD, Selenof KO ND, and Selenof KO WD Cohorts.** Mice were weighed weekly, and age matched. The average weight for that age was graphed. For each cohort, n=10. Selenof KO ND vs Selenof KO WD,  $p < 0.0001$ . WT ND vs WT WD,  $p < 0.0001$ . Selenof KO WD vs WT WD,  $p < 0.0001$ . Two-way ANOVA was used. There was no significant difference between the starting weights.

### Fasting Glucose Measurements

The average fasting glucose measurement was calculated for each cohort at 3 time points: the first around 6 weeks of age (before challenge with DMBA or WD), the second between 11 and 17 weeks of age (after finishing the DMBA protocol), and a third after 18 weeks of age (Figure 9). Due to the suddenness of reaching end-point criteria in the Selenof KO WD cohort, only one measurement was taken after 18 weeks of age. While not reaching statistical significance, there is a trend of increased fasting blood glucose level in the Selenof KO cohorts compared to the WT cohorts, this is present even prior to DMBA administration and diet intervention (Figure 9). This trend continues after DMBA exposure and diet intervention (Figure

9). With diet intervention, the WT WD and Selenof KO WD cohorts show a trend in fasting glucose elevation compared to the WT ND and Selenof KO ND cohorts (Figure 9).

Interestingly, even without the WD challenge, the Selenof KO ND cohort shows a trend in increasing fasting blood glucose compared to the WT ND (Figure 9). The Selenof KO WD cohort's fasting glucose levels show a trend in increasing compared to the WT WD cohort (Figure 9). While the overall trend of the Selenof KO cohorts' increased fasting glucose compared to the WT cohorts' does not reach statistical significance, it is intriguing and warrants further and more comprehensive studies.

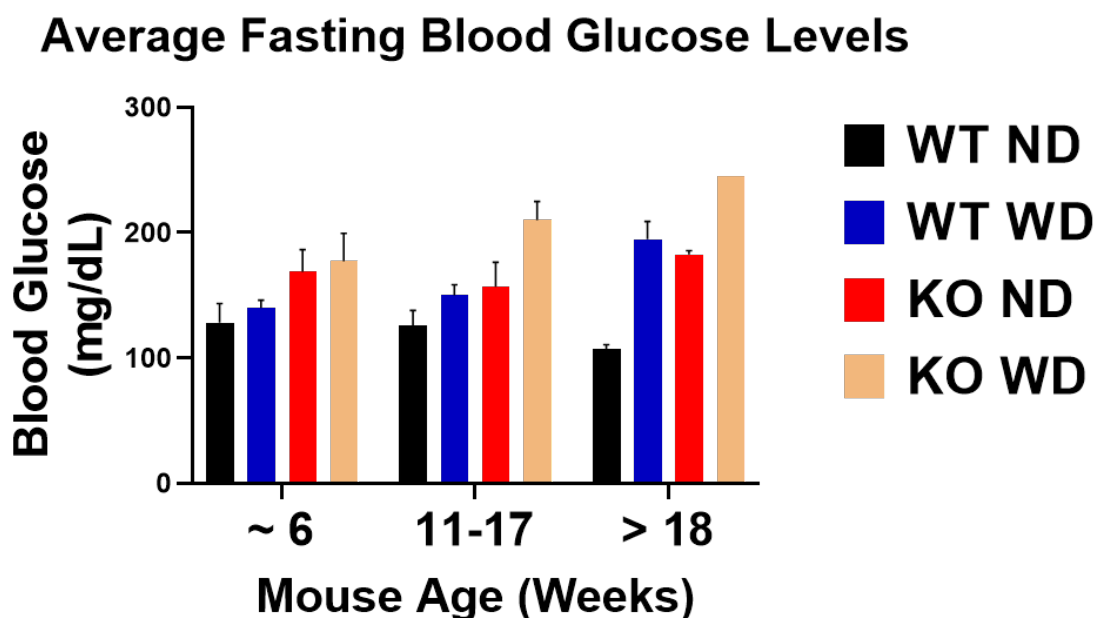


**Figure 9. Average Fasting Blood Glucose Measurements of Mice.** Three glucose measurements were taken after an overnight fast. While not reaching statistical significance, there is a trend of increasing fasting blood glucose in the Selenof KO ND and WD cohort older than 18 weeks.

### Overall Tumor Burden

All tumors were counted when the mice reached end-point criteria as determined by IACUC guidelines or when the study concluded. Lesions were sent to Dr. Maarten Bosland at University of Illinois Chicago (UIC) for confirmation and analysis. Images of representative tumors are shown in Figures 11 to 13.

Many mice had multiple tumors; the number of tumors, total and stratified by organ type, are shown in Tables 1 and 2. A lymphoma was counted as one tumor, regardless of how many lymphoma deposits were found by pathology. Benign papilloma on the skin were counted as tumors in addition to squamous cell carcinoma lesions [54]. The number of tumors (tumor multiplicity), regardless of type, was graphed for each animal and the cohorts were compared using an Unpaired t test with Welch's Correction (Figure 10A-C). The tumor multiplicity for the SELENOF KO ND and SELENOF KO WD cohort was higher than the WT ND cohort (Figure 12A). However, the WD alone did not significantly increase the total tumor multiplicity in WT mice or in the context of Selenof loss (Figure 10A-C). This data indicates that the loss of Selenof alone increases tumor multiplicity *in vivo*.

We noted that many tumors originated from the skin (Figure 10C). Therefore, we graphed tumor multiplicity for tumors originating from the skin only (Figure 10C) and for tumors originating from any other organ (Figure 10B) to determine how much of the tumor burden was due to skin tumors. Representative images of skin lesions are shown in Figure 13 and Figure 14. When only tumor multiplicity due to skin tumors was graphed, Selenof KO ND and Selenof KO WD mice had significantly increased tumor multiplicity compared to WT ND mice (Figure 10C). These data indicates that while a WD challenge was not enough to increase skin tumor multiplicity, the loss of Selenof is (Figure 10A-C). This is similar to the results from the total

tumor multiplicity (Figure 10C). When tumors originating from the skin were removed from the data, as in Figure 13 and Figure 14, there is no difference in tumor multiplicity between the 4 cohorts. These data indicate that our study's difference in tumor multiplicity is largely due to skin tumors.

Due to the increase in skin tumorigenesis seen in our Selenof KO cohorts, we took skin biopsies of DMBA naïve Selenof KO and WT mice to elucidate if there was a phenotypic difference prior to a chemical carcinogen challenge. We took a total of 16 biopsies from 4 Selenof KO mice and 12 biopsies from 3 WT mice. Examination by pathology revealed no abnormalities or differences between the Selenof KO and WT biopsies (data not shown).

**Table 1. Number of Mice with Tumors at End-Point, Stratified by Organ.** Of note: In the WT ND cohort, one mouse had both a skin tumor and lymphoma. In the WT WD cohort, one mouse had a skin tumor and lymphoma and one mouse had a mammary tumor and mammary metastasis (counted as “Other”). In the Selenof KO ND cohort, one mouse had a skin tumor and ovarian tumor and one mouse had a skin tumor and lymphoma. In the Selenof KO WD cohort, one mouse had a skin tumor and mammary tumor, and one mouse had a skin tumor and lymphoma.

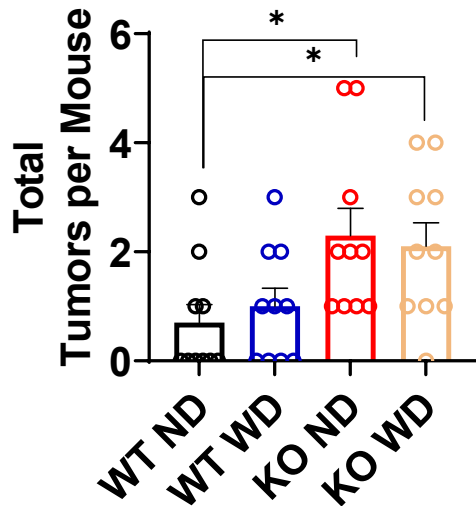
Cohort	Mice, N	Mammary	Skin	Lymphoma	Other	Total
WT, ND	10	0	3	2	0	3
WT, WD	10	1	4	2	1	6
Selenof KO, ND	10	0	10	1	1	10
Selenof KO, WD	10	1	8	2	0	9

**Table 2. Number of Tumors in Each Cohort at End-Point, Stratified by Organ.**

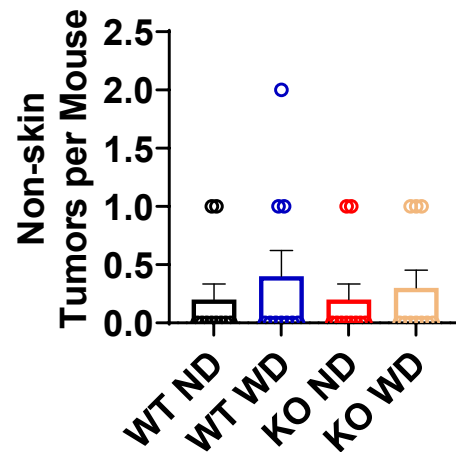
Cohort	Mice, N	Mammary	Skin	Lymphoma	Other	Total
WT, ND	10	0	5	2	0	7
WT, WD	10	1	6	2	1	9
Selenof KO, ND	10	0	21	1	1	23
Selenof KO, WD	10	1	18	2	0	21



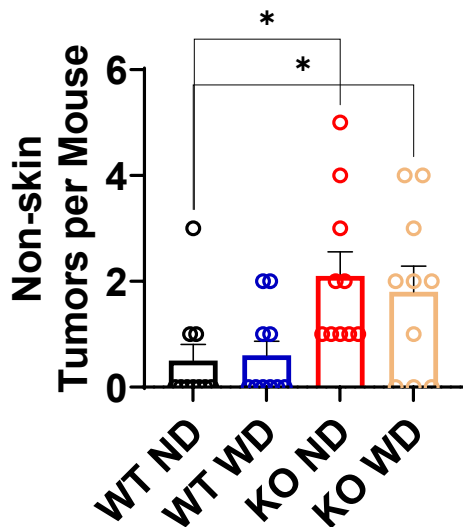
### A. Tumors Multiplicity (Total)



### B. Non-skin Tumor Multiplicity

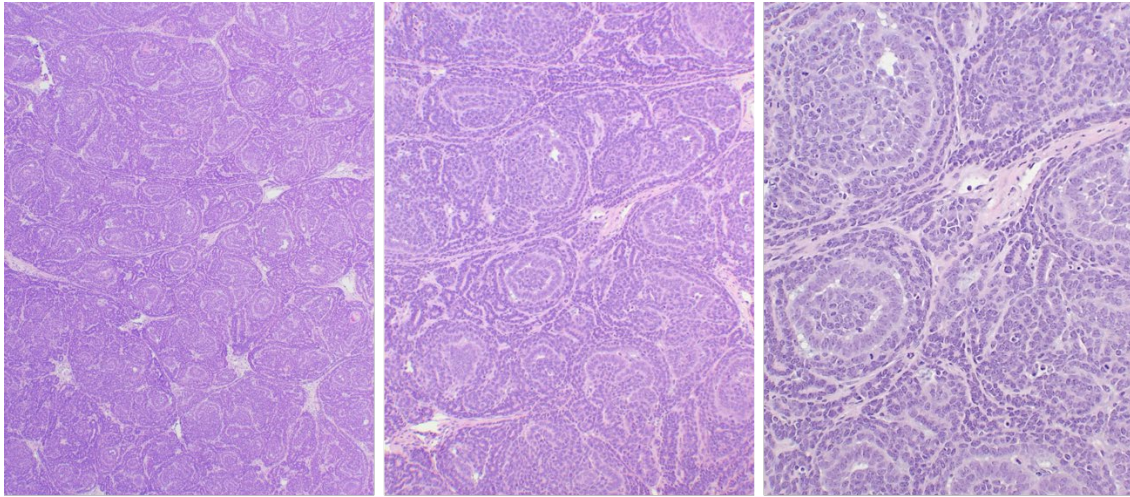


### C. Skin Only Tumor Multiplicity



### Figure 10. Increased Tumor Multiplicity in Selenof KO Mice is Largely Due to Skin Tumors.

A) Graph of overall tumor multiplicity, including tumors originating from any organ WT ND vs KO ND,  $p=0.025$  and for WT ND vs KO WD,  $p=0.017$ . Unpaired t test with Welch's Correction was used. B) Graph of tumor multiplicity for only tumors not originating from the skin. Significance disappears when skin tumors are taken out of the graph. C) Graph of tumor multiplicity for tumors originating from the skin only. WT ND vs KO ND,  $p=0.011$  and for WT ND vs KO WD,  $p=0.05$ . Unpaired t test with Welch's Correction was used.

**A.**

Low power (4x)

Medium power (10X)

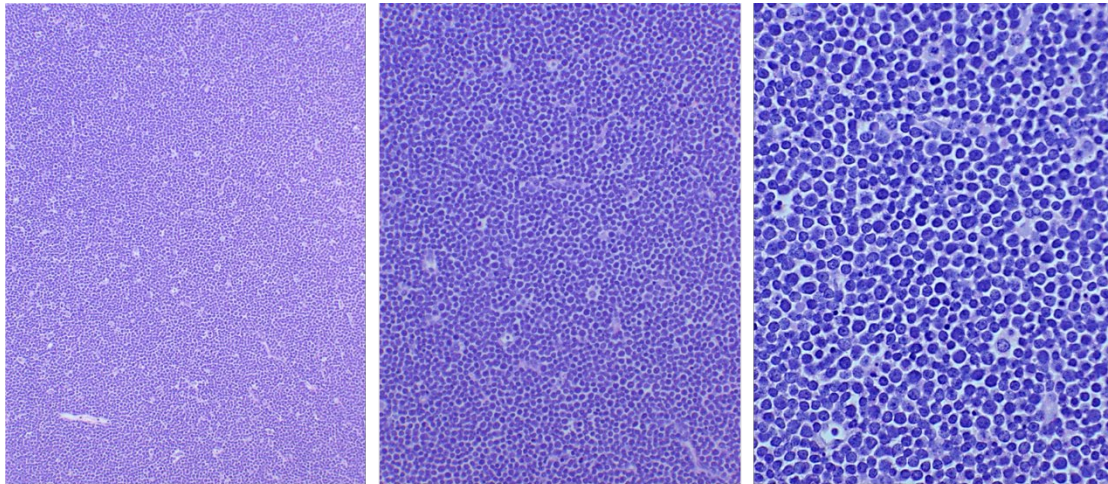
High Power (20x)

Mammary Gland Tubular Adenocarcinoma

**B.**

Rare Pulmonary Metastasis of Mammary Gland Adenocarcinoma

**Figure 11. Representative H&E Slide of Mammary Tumors.** Representative hematoxylin and eosin (H&E) stained slide of the murine mammary tumors observed. A) A mammary gland tubular adenocarcinoma shown at 4x, 10x, and 20x B) A rare pulmonary metastasis of a mammary gland adenocarcinoma shown.



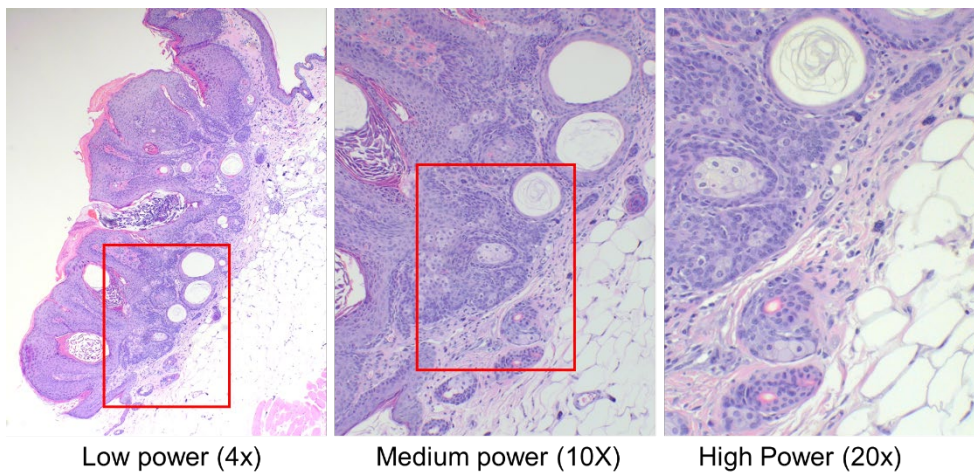
Low power (4x)

Medium power (10X)

High Power (20x)

Thymus Lymphocytic Lymphoma

**Figure 12. Representative H&E Slide of a Thymus Lymphocytic Lymphoma.** Thymus lymphocytic lymphoma hematoxylin and eosin (H&E) stained slide shown at 4x, 10x, and 20x.

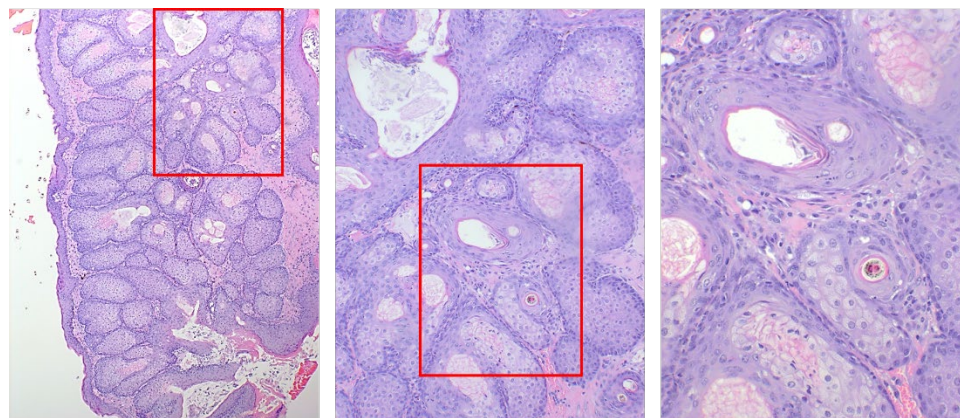
**A.**

Low power (4x)

Medium power (10X)

High Power (20x)

Skin Early Stage Sebaceous-Squamous Cell Carcinoma

**B.**

Low power (4x)

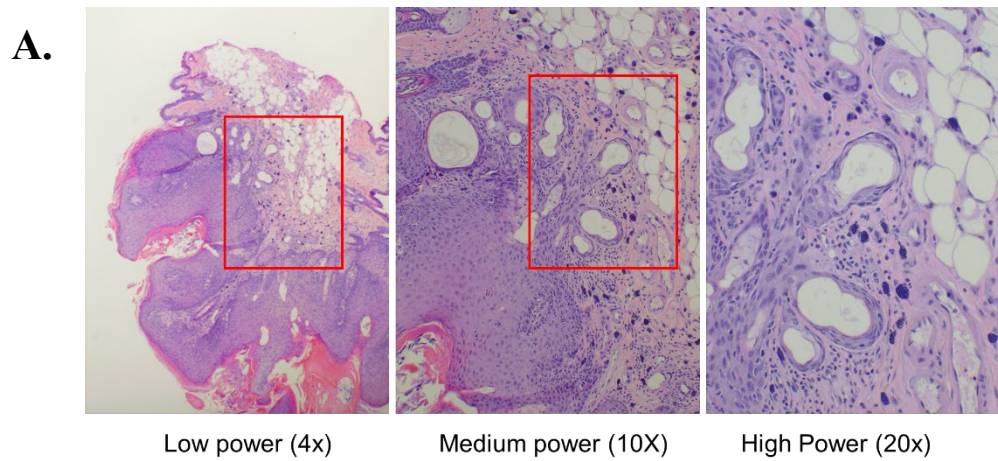
Medium power (10X)

High Power (20x)

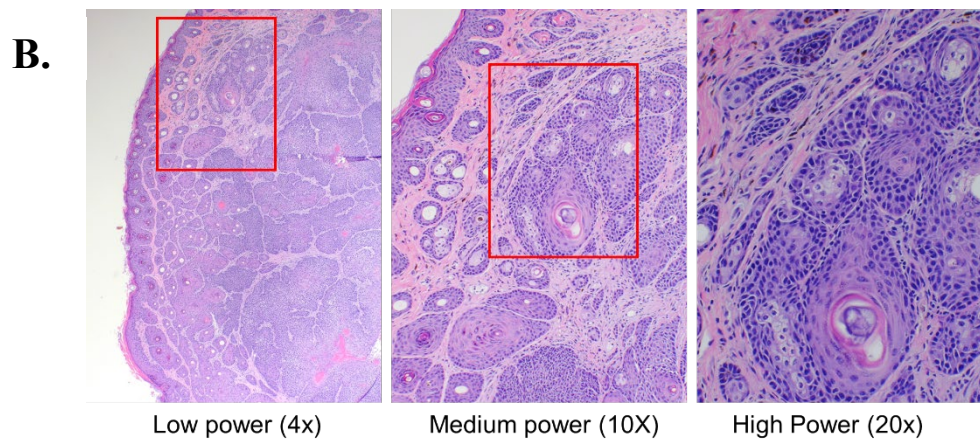
Skin Sebaceous-Squamous Cell Carcinoma

**Figure 13. Representative H&E Slides of Sebaceous-Squamous Cell Carcinomas.**

Representative hematoxylin and eosin (H&E) stained slides of the skin tumors observed, confirmed to be squamous cell carcinoma A) Early stage sebaceous-squamous cell carcinoma shown at 4x, 10x, and 20x. B) Sebaceous-squamous cell carcinoma shown at 4x, 10x, and 20x. Figure continues, page 36.



Skin Early Stage Squamous Cell Carcinoma



Skin Squamous Cell Carcinoma

**Figure 14. Representative H&E Slides of Squamous Cell Carcinomas.** A) Early-stage squamous cell carcinoma shown at 4x, 10x, and 20x. B) Squamous cell carcinoma shown at 4x, 10x, and 20x.

### **Tumor Incidence**

The tumor incidence was tracked for all mice and plotted on a Kaplan-Meier graph (Figure 15A). At the timepoint when the first tumor was seen on a mouse, it was counted as an event in the Kaplan-Meier plot (Figure 15A). A Log-Rank Mantel Cox test was used to evaluate tumor incidence between the WT ND, WT WD, Selenof KO ND, and Selenof KO WD cohorts (Figure 15A-B). At 25 weeks after the DMBA protocol, there was a significant difference in the percentage of mice that developed tumors between the WT ND and Selenof KO ND cohorts ( $p = 0.0058$ ) and between the WT ND and Selenof KO WD cohorts ( $p = 0.0012$ ) (Figure 15A). Of note, there was one Selenof KO ND mouse and one WT ND mouse that did not develop a tumor until after 25-week cut off. These mice are included in the total percentage of mice that developed tumors in Table 1.

### **Mammary Tumorigenesis**

Only one Selenof KO mouse developed a mammary tumor, and this mouse was in the WD cohort (Table 1 and 2). Similarly, only one WT mouse developed a mammary tumor, also in the WD cohort (Table 1 and 2). There was no significant difference in the number of mammary tumors developed between any of the cohorts. Representative images are shown in Figure 11. While this data indicates WD may cause a trend to increase mammary tumor incidence, independent of genotype.

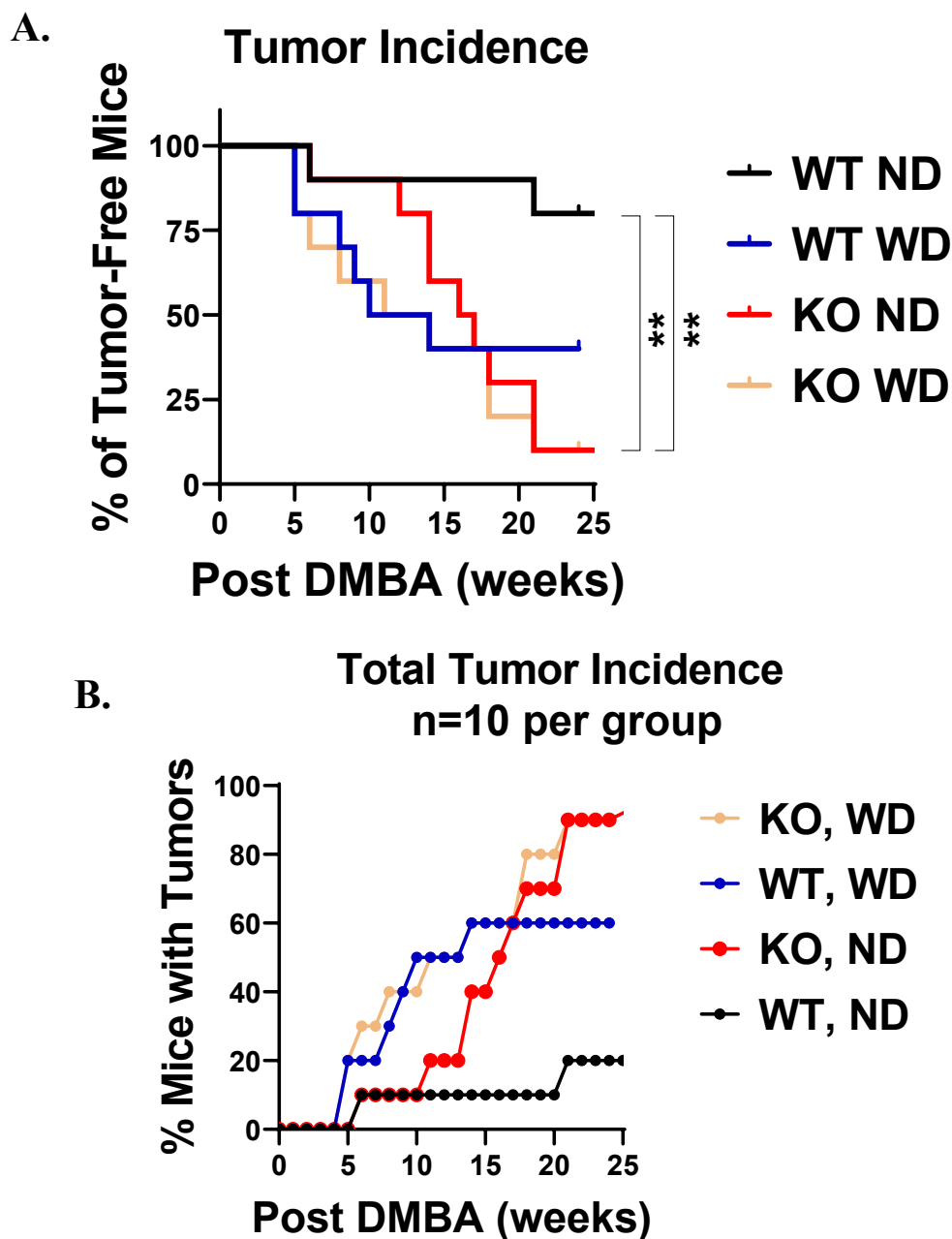


**Figure 15. Tumor Incidence is Increased in Selenof KO Mice** A) Percent of tumor-free mice over the number of weeks after DMBA exposure shown with a Kaplan-Meier plot. Selenof KO ND vs WT ND,  $p=0.0058$  and Selenof KO WD vs WT ND,  $p=0.0012$ . Log rank (Mantel-Cox) test was used. The same data as in A shown as percent of mice with tumors over the number of weeks after DMBA exposure.

## CHAPTER III

### DISCUSSION

This project aimed to determine whether the loss of Selenof in combination with a Western diet (WD) promotes mammary tumorigenesis in a mouse model. We did not find a significant difference in mammary tumorigenesis between the Selenof KO and WT cohorts, though only mice in the WD cohorts developed mammary tumors (Tables 1 and 2). Our results may indicate a contribution from the diet, however too few mammary tumors occurred to make any conclusions. While the expected rate of mammary tumorigenesis was 30-70% per Plante (2021), less than 30% of the mice in our study developed mammary tumors [42].

There are a few possibilities for why less than 30% of our total mouse population developed mammary tumors. The first possibility is differences in the sensitivities of mouse strains to DMBA. Our study used C57Bl/6 mice, while the DMBA protocol referenced used FVB/N mice [42]. Additionally, Hudson et al. had previously noted only 22.5% of WT C57Bl/6 background mice developed DMBA-induced mammary tumors compared to 42.5% of WT FVB/N background mice and that FVB/N background mice developed mammary tumors sooner [28]. For our study, we used C57Bl/6 background mice, as this was the strain Kasaikina et al. developed the Selenof KO model in [51]. It is feasible that the strain impacted the rate of mammary tumor formation in our study [28, 40].

We know that hormone levels are required for mammary tumorigenesis, and pregnancy, which yields high hormone levels, has been shown to increase the incidence of mammary tumors



in mice and some studies use pregnancy to increase mammary tumor incidence [55]. However, the mice in our study were not pregnant and had never been pregnant. To increase the incidence of mammary tumors in the future, we could consider adding a male after DMBA treatment is finished for the duration of multiple pregnancies.

An unexpected finding of our study was the increased skin tumor incidence and multiplicity in the Selenof KO cohorts compared to the WT cohorts. According to the Human Protein Atlas, SELENOF levels are medium in the skin (<https://www.proteinatlas.org/ENSG00000183291-SELENOF>). While we did take biopsies of DMBA naïve mice (which were not part of the study) to determine if there was any indication of transformation in the skin in Selenof KO mice, pathology did not note any differences upon examination of H&E slides. The observed phenotype of increased skin tumorigenesis warrants further investigation.

The early termination in the study due to tumor burden from skin lesions also may have negatively impacted the mammary tumor incidence. Of note, mammary tumorigenesis should take 30-40 weeks post DMBA to develop. Still, we had to terminate at 25 weeks post DMBA because many mice reached end-point criteria early due to skin lesions and lymphomas. To avoid the compounding factor of tumor burden developing in other sites, we propose an organoid model of mammary glands [54]. In an organoid model, mammary glands from WT and Selenof KO mice would be treated with DMBA [54]. Additionally, in the controlled environment of an organoid model, mammary glands could be closely examined for signs of transformation with the loss of Selenof. Another model to avoid tumor burden from organs other than the mammary gland would be a mammary specific Selenof KO. Hudson et al used murine mammary tumor

virus (MMTV) to knockout *Trsp* in the mammary glands only, this same method could be used to create a mammary gland specific Selenof KO [28].

While a previous study had indicated that a loss of Selenof resulted in increased body weight when challenged with a WD, this was not the case in our study [36]. The Selenof KO mice in our study had less weight gain than the WT mice, both in the ND and WD cohort (Figure 8). One possibility is that there was a higher overall tumor burden (measured by total number of tumors) in the KO cohort than the WT cohort and that this tumor burden affected the weight gain. The previous study by Zheng et al. (2020) which showed increased weight gain in Selenof KO mice on a high-fat (Western) diet did not challenge mice with a chemical carcinogen or genetic model [36]. There was no DMBA naïve cohort of WT or Selenof KO mice, which limited us from determining if the tumor burden or DMBA itself impacted the weight gain of the mice. One option to rule out the possibility that tumor burden impacts the ability of the mice in our study to gain weight would be to start the mice on the WD prior to administering DMBA. However, this would likely affect mammary tumor development efficiency since DMBA needs to be administered when the mammary gland is undergoing the highest rate of proliferation and is most sensitive to the carcinogenic insult [42-44].

Additionally, our study used only female mice, while the Zheng et al. (2020) exclusively used male mice [36]. Female mice have been shown to be less sensitive to a Western (high fat) diet causing weight gain due to circulating estrogen levels [56, 57]. While ovariectomizing the female mice would decrease estrogen levels and the expectation would be that they would gain weight similarly to the male counterparts in the previous study, this would have been counterproductive to the purpose of the study to examine mammary tumorigenesis as estrogen is required for mammary tumorigenesis [36, 42]. We did, however, note a trend in increasing

fasting glucose levels in the Selenof KO cohorts, which is consistent with previous studies [36]. It is yet to be determined if the increases in blood glucose levels are related to the increased overall tumorigenesis in the Selenof KO mice.

### **Conclusion**

While the study was inconclusive regarding mammary tumors, more Selenof KO mice developed tumors compared to WT mice and the tumor burden was higher in the Selenof KO cohorts. A large amount of tumor burden was due to skin tumors, consisting of benign papilloma and squamous cell carcinoma. The addition of the WD caused a trend in an increased overall tumor burden in the WT and Selenof KO cohorts as well as in mammary tumorigenesis. Proposed future studies to better investigate mammary tumorigenesis include a mammary gland-specific knockout or an organoid model. Additional studies on the putative role of SELENOF and skin cancer are warranted based on our observation of significant increases in skin tumorigenesis in the Selenof KO cohorts.

While the loss of Selenof did not cause an increase in weight gain, there was a trend in increase fasting glucose measurements, indicating metabolic dysfunction. This warrants further, more in-depth studies of the effect that loss of SELENOF may have on metabolic dysfunction as well as to elucidate if this is a distinct phenotype from tumorigenesis, or if the two are linked. Overall, our findings in these loss-of-function studies are consistent with the notion that SELENOF is a tumor suppressor.

CHAPTER IV  
MATERIALS AND METHODS

**Selenof Knockout Mice**

Selenof knockout (KO) mice were obtained from our collaborator Dr. Alan Diamond at University of Illinois – Chicago, which were then used to start our own colony. Female mice from our Selenof KO colony were used for the study and randomized into the WD or ND cohort. The Selenof KO mice were originally generated by Kasaikina et al. (2011) using a Neo cassette with transcript terminators to replace exon 2 in the *Selenof* gene which resulted in no functional or truncated Selenof, undetectable by an immunoprecipitation blot [53]. Selenof KO mice showed no overt phenotype or change in body weight compared to WT mice [35, 53]. Please see Kasaikina et al. (2011) for complete details regarding the development of the systemic Selenof KO mice used in this study [53].

**Mouse Housing and Diets**

Mice used in the protocol were housed in the Loyola University Chicago Cardinal Bernardine Cancer Center mouse facilities and experiments were conducted in accordance with institutional procedures and guidelines after approval from the Institutional Animal Care and Use Committee (IACUC). The housing facilities were on a 12-hour light/dark cycle and all mice were provided food and water at liberty.

Mice placed in the Normal Diet (ND) cohort were fed the normal chow provided by Loyola University Chicago Health Sciences Campus Comparative Medicine Facility (CMF) which has 17% calories from fat, 58% calories from carbohydrates, 25% calories from protein

and energy density of 3.1 kcal/g (<https://www.inotivco.com/rodent-traditional-natural-ingredient-diets>, catalog number: 7912, irradiated). Mice in the ND cohort were fed the ND at liberty for the entirety of the time in the study. Mice placed in the Western Diet (WD) cohort were fed “Western” purified atherogenic diet from Envigo, catalog number TD.88137 which has 42% calories from fat, 42% calories from carbohydrates, 15.2% calories from protein, and energy density of 4.5 kcal/g (<https://www.inotivco.com/atherogenic-custom-diets>). Selenium levels are the same in both diets. Mice in the WD cohort were fed the WD at liberty for the entirety of the time in the study.

### **DMBA Preparation and Protocol**

7,12-dimethylbenz[a]anthracene (DMBA) was reconstituted by adding one milliliter of corn oil per 10 milligrams of powder DMBA and heating to 37 degrees Celsius while stirring and covering with foil to prevent exposure to light [42]. Reconstituted DMBA was kept at 4 degrees Celsius in amber glass vials for the entirety of the protocol [42]. Mice were fed 100 microliters of the reconstituted DMBA in corn oil (for a final concentration of 1mg DMBA) weekly for six weeks, starting at approximately six weeks old [42].

### **Weight, Lesion, and Glucose Measurements**

Glucose measurements were taken in the morning, after an overnight fast with an animal glucometer (1AlphaTRAK2 Blood Glucose Monitoring Meter and corresponding test strips). Three glucose measurements were taken, one before mice were randomized into their respective diet cohorts or DMBA (approximately 6 weeks old), one after they had finished the protocol (approximately 12 weeks old), and one final time point when mice had been finished with the DMBA protocol for multiple weeks (18 weeks and older). All mice were weighed weekly, and

weights were recorded in grams. Palpable and measurable lesions were measured with calipers on a weekly basis and recorded in millimeters.

### **Sample Preparation and Analysis**

Lesions seen upon necropsy were isolated, placed in cassettes, and submerged in 10% neutral buffered formalin for 24 hours, after which samples were washed with phosphate buffered saline (PBS) three times and left submerged in PBS with two milliliters of 4% paraformaldehyde until samples were sent for paraffin embedding, slide mounting, and Hematoxylin and Eosin (H&E) staining (up to one week later). Stained slides were then sent to Dr. Maarten Bosland at University of Illinois at Chicago for histologic evaluation.

### **Genotyping**

Genotyping to confirm the complete systemic loss of *Selenof* in our *Selenof* KO mice and the presence of *Selenof* in the WT mice was done using tissue from tail snips. Tail snips of 5 millimeters were taken the same day mice started the DMBA protocol, at approximately six weeks old. Tail snips were stored at -20 degrees Celsius until the tissue extraction protocol. Tissue extraction and PCR protocol were done with the REDEExtract-N-Amp™ kit from Sigma-Aldrich (catalog number: XNAT-100RXN) using 25uL of extraction solution and 6.25uL of tissue preparation solution placed into a microcentrifuge tube with tail, cut side down. Samples were then incubated for 10min at 95C, after which 25uL of Neutralization buffer was added. Samples were stored at -20 degrees Celsius until REDEExtract PCR protocol was performed. Primers were ordered from Integrated DNA Technologies. To detect *Selenof* presence, the reverse *Selenof* primer (TTT GGC CAG ATA CCA GGA AG) and forward *Selenof* primer (GCA GCT CTT GCG ATC TTC TT) were used [35, 53]. Since *Selenof* KO mice would not have a SELENOF band present, a band for the presence of the Neo cassette was used as a positive

control [35, 53]. To detect the presence of a Neo cassette band, the Neo forward primer (TCG CCT TCT TGA CGA GTT CT) and *Selenof* reverse primer were used, as in Kasaikina et al. (2011) [35, 53]. Tissue extract, REExtract and corresponding primer mix were combined to a volume of 20 $\mu$ L and placed in the thermal cycler (see Table 3 for full protocol). The samples were then run on a 1% agarose gel with SYBR<sup>TM</sup> Safe DNA gel stain and visualized using UV (results in Figures 6 and 7).

**Table 3. Thermal Cycler Protocol for Genotyping.**

Step	Temperature	Time	Number of Cycles
<b>Initial Denaturation</b>	94C	3 minutes	1
<b>Denaturation</b>	94C	45 seconds	35
<b>Annealing</b>	52C	45 seconds	35
<b>Extension</b>	72C	1.5 minutes	35
<b>Final Extension</b>	72C	10 minutes	1
<b>Hold</b>	4C	$\infty$	

### Western Blot

Western blot for *Selenof* was performed on the mammary glands of representative DMBA treated and DMBA naïve age-matched *Selenof* KO and WT mice. Normal mammary glands were collected from DMBA treated *Selenof* KO and WT mice when mice completed the study. Normal mammary glands were collected from *Selenof* KO and WT mice that were never exposed to DMBA when mice were approximately 24 weeks old. Mammary glands were snap frozen in liquid nitrogen when collected and then stored at -80 degrees Celsius until lysate preparation protocol was performed. Lysate preparation protocol was adapted from ThermoFisher Scientific. Lysis buffer was prepared using 90% T-PER, 5% Protease Inhibitor, and 5% PhosStop. For every 50mg of tissue, 500 $\mu$ L of lysis buffer was used. Protein

concentration was determined using a bicinchoninic acid (BCA) assay. For the Western Blot, 60ug of protein was loaded into each well and run on a 10% acrylamide SDS-PAGE. Proteins were transferred onto PVDF membranes using an iBlot 2 instrument. After transfer, membranes were blocked with 5% milk in TBS-T for 1 hour before blocking with the appropriate primary antibody overnight, followed by blocking with the secondary antibody for 1 hour. Membranes were imaged immediately following using an iBright CL100 Imaging system with Pierce Suprasignal West Pico chemiluminescent substrate from ThermoFisher.

### **RT-quantitative PCR (QPCR)**

QPCR was used to measure *Selenof* mRNA levels in the mammary glands of WT C57Bl/6 mice and *Selenof* KO mice (C57Bl/6 background). The RNA was isolated using Qiagen's RNeasy Lipid Tissue Mini Kit (catalog number: 74804). Mammary glands were taken from *Selenof* KO and WT mice. RNA was isolated according to the Qiagen RNeasy Lipid Tissue Mini Kit (catalog number: 74804) instructions. After RNA isolation, 0.5ug of RNA in a volume of 10uL was reverse transcribed using 200U of M-MLV reverse transcriptase, 100ng random hexamer, 0.5mM deoxy-NTP, and 10mMDTT. The cDNA from the reverse transcriptase reaction was then added to a SYBER Green Master Mix containing the appropriate forward and reverse primers and amplified using a ThermoFisher Scientific QuantStudio3. The fold change was calculated using  $\Delta\Delta C_t$ , using  $\beta$ -actin as the control. If fold change was unable to be graphed due to a lack of amplification after 40 cycles, the average number of cycles was used.

### **3D Acinar Assay**

The 3D acinar assay protocol used was adapted from the protocol developed by Lee et al, 2007 [58]. Plates were coated with 200uL of Corning Matrigel basement membrane matrix and incubated at 37 degrees Celsius for 30 minutes. Single cell suspension of  $1.5 \times 10^4$  cells in



10% Matrigel were plated on the coated wells. After which, 150uL of culture medium was added every 48 hours for the 20-day growth period. The 3D acini were stained with Propidium Iodide (P.I.), Hoechst 33342 (Hoechst), and Calcein AM in the dark for 20 minutes. Images were acquired using a Nikon inverted fluorescence microscope.

### **Statistical Analysis**

Data are presented as mean + or – the Standard Error of the Mean (SEM) from 3 biological replicates unless otherwise stated. Statistical analysis consisted of 2-way ANOVA, Unpaired students t test, or Log-Rank (Mantel-Kox) as appropriate. Statistical analyses were done using GraphPad Prism 9.

## REFERENCE LIST

1. Siegel, R.L., et al., *Cancer statistics, 2022*. CA Cancer J Clin, 2022. **72**(1): p. 7-33.
2. Flowers, B., A. Poles, and I. Kastrati, *Selenium and breast cancer - An update of clinical and epidemiological data*. Arch Biochem Biophys, 2022. **732**: p. 109465.
3. Cortesi, L., H.S. Rugo, and C. Jackisch, *An Overview of PARP Inhibitors for the Treatment of Breast Cancer*. Target Oncol, 2021. **16**(3): p. 255-282.
4. Rayman, M.P., *Selenium in cancer prevention: a review of the evidence and mechanism of action*. Proc Nutr Soc, 2005. **64**(4): p. 527-42.
5. Rayman, M.P., *Selenium intake, status, and health: a complex relationship*. Hormones (Athens), 2020. **19**(1): p. 9-14.
6. Zigrossi, A., et al., *SELENOF is a new tumor suppressor in breast cancer*. Oncogene, 2022. **41**(9): p. 1263-1268.
7. Diwadkar-Navsariwala, V. and A.M. Diamond, *The link between selenium and chemoprevention: a case for selenoproteins*. J Nutr, 2004. **134**(11): p. 2899-902.
8. Lippman, S.M., et al., *Effect of selenium and vitamin E on risk of prostate cancer and other cancers: the Selenium and Vitamin E Cancer Prevention Trial (SELECT)*. JAMA, 2009. **301**(1): p. 39-51.
9. Pierce, J.P., et al., *A randomized trial of the effect of a plant-based dietary pattern on additional breast cancer events and survival: the Women's Healthy Eating and Living (WHEL) Study*. Control Clin Trials, 2002. **23**(6): p. 728-56.
10. Saquib, J., et al., *Dietary intake, supplement use, and survival among women diagnosed with early-stage breast cancer*. Nutr Cancer, 2011. **63**(3): p. 327-33.

11. Bengtsson, Y., M. Sandsveden, and J. Manjer, *Risk of breast cancer in relation to dietary intake of selenium and serum selenium as a marker of dietary intake: a prospective cohort study within The Malmo Diet and Cancer Study*. *Cancer Causes Control*, 2021. **32**(8): p. 815-826.
12. Charalabopoulos, K., et al., *Selenium in serum and neoplastic tissue in breast cancer: correlation with CEA*. *Br J Cancer*, 2006. **95**(6): p. 674-6.
13. Guo, D., et al., *Association between selenium intake and breast cancer risk: results from the Women's Health Initiative*. *Breast Cancer Res Treat*, 2020. **183**(1): p. 217-226.
14. Lubinski, J., et al., *Serum selenium levels predict survival after breast cancer*. *Breast Cancer Res Treat*, 2018. **167**(2): p. 591-598.
15. Szwiec, M., et al., *Serum Selenium Level Predicts 10-Year Survival after Breast Cancer*. *Nutrients*, 2021. **13**(3).
16. Ekoue, D.N., et al., *Correlations of SELENOF and SELENOP genotypes with serum selenium levels and prostate cancer*. *Prostate*, 2018. **78**(4): p. 279-288.
17. Xun, P., et al., *Distribution of toenail selenium levels in young adult Caucasians and African Americans in the United States: the CARDIA Trace Element Study*. *Environ Res*, 2011. **111**(4): p. 514-9.
18. Colditz, G.A., *Epidemiology of breast cancer. Findings from the nurses' health study*. *Cancer*, 1993. **71**(4 Suppl): p. 1480-9.
19. Pierce, J.P., *Diet and breast cancer prognosis: making sense of the Women's Healthy Eating and Living and Women's Intervention Nutrition Study trials*. *Curr Opin Obstet Gynecol*, 2009. **21**(1): p. 86-91.
20. Demircan, K., et al., *Serum selenium, selenoprotein P and glutathione peroxidase 3 as predictors of mortality and recurrence following breast cancer diagnosis: A multicentre cohort study*. *Redox Biol*, 2021. **47**: p. 102145.
21. Sandsveden, M., et al., *Prediagnostic serum selenium levels in relation to breast cancer survival and tumor characteristics*. *Int J Cancer*, 2020. **147**(9): p. 2424-2436.

22. Berry, M.J., et al., *Recognition of UGA as a selenocysteine codon in type I deiodinase requires sequences in the 3' untranslated region*. *Nature*, 1991. **353**(6341): p. 273-6.
23. Arner, E.S., *Selenoproteins-What unique properties can arise with selenocysteine in place of cysteine?* *Exp Cell Res*, 2010. **316**(8): p. 1296-303.
24. Labunskyy, V.M., et al., *Sep15, a thioredoxin-like selenoprotein, is involved in the unfolded protein response and differentially regulated by adaptive and acute ER stresses*. *Biochemistry*, 2009. **48**(35): p. 8458-65.
25. Hatfield, D.L., et al., *Selenium and selenocysteine: roles in cancer, health, and development*. *Trends Biochem Sci*, 2014. **39**(3): p. 112-20.
26. Hatfield, D.L. and V.N. Gladyshev, *How selenium has altered our understanding of the genetic code*. *Mol Cell Biol*, 2002. **22**(11): p. 3565-76.
27. Labunskyy, V.M., D.L. Hatfield, and V.N. Gladyshev, *Selenoproteins: molecular pathways and physiological roles*. *Physiol Rev*, 2014. **94**(3): p. 739-77.
28. Gladyshev, V.N., et al., *Selenoprotein Gene Nomenclature*. *J Biol Chem*, 2016. **291**(46): p. 24036-24040.
29. Hudson, T.S., et al., *Selenoproteins reduce susceptibility to DMBA-induced mammary carcinogenesis*. *Carcinogenesis*, 2012. **33**(6): p. 1225-30.
30. Nagai, H., et al., *Detection and cloning of a common region of loss of heterozygosity at chromosome 1p in breast cancer*. *Cancer Res*, 1995. **55**(8): p. 1752-7.
31. Gladyshev, V.N., et al., *A new human selenium-containing protein. Purification, characterization, and cDNA sequence*. *J Biol Chem*, 1998. **273**(15): p. 8910-5.
32. Ferguson, A.D., et al., *NMR structures of the selenoproteins Sep15 and SelM reveal redox activity of a new thioredoxin-like family*. *J Biol Chem*, 2006. **281**(6): p. 3536-43.
33. Hong, L.K., et al., *Loss of SELENOF Induces the Transformed Phenotype in Human Immortalized Prostate Epithelial Cells*. *Int J Mol Sci*, 2021. **22**(21).

34. Hu, Y.J., et al., *Distribution and functional consequences of nucleotide polymorphisms in the 3'-untranslated region of the human Sep15 gene*. *Cancer Res*, 2001. **61**(5): p. 2307-10.
35. Yim, S.H., et al., *Role of Selenof as a Gatekeeper of Secreted Disulfide-Rich Glycoproteins*. *Cell Rep*, 2018. **23**(5): p. 1387-1398.
36. Zheng, X., et al., *Selenoprotein F knockout leads to glucose and lipid metabolism disorders in mice*. *J Biol Inorg Chem*, 2020. **25**(7): p. 1009-1022.
37. Zhang, D.G., et al., *Selenoprotein F (SELENOF)-mediated AKT1-FOXO3a-PYGL axis contributes to selenium supranutrition-induced glycogenolysis and lipogenesis*. *Biochim Biophys Acta Gene Regul Mech*, 2022. **1865**(3): p. 194814.
38. Flowers, B., et al., *Distinct Roles of SELENOF in Different Human Cancers*. *Biomolecules*, 2023. **13**(3).
39. Garcia-Estevez, L., et al., *Obesity and Breast Cancer: A Paradoxical and Controversial Relationship Influenced by Menopausal Status*. *Front Oncol*, 2021. **11**: p. 705911.
40. Neuhouser, M.L., et al., *Overweight, Obesity, and Postmenopausal Invasive Breast Cancer Risk: A Secondary Analysis of the Women's Health Initiative Randomized Clinical Trials*. *JAMA Oncol*, 2015. **1**(5): p. 611-21.
41. Kerdelhue, B., C. Forest, and X. Coumoul, *Dimethyl-Benz(a)anthracene: A mammary carcinogen and a neuroendocrine disruptor*. *Biochim Open*, 2016. **3**: p. 49-55.
42. Plante, I., *Dimethylbenz(a)anthracene-induced mammary tumorigenesis in mice*. *Methods Cell Biol*, 2021. **163**: p. 21-44.
43. Rajapaksa, K.S., *11.23 - Ovarian Metabolism of Xenobiotics*. *Comprehensive Toxicology (Second Edition)*, 2010: p. 457-467.
44. Helena, J.M., et al., *Deoxyribonucleic Acid Damage and Repair: Capitalizing on Our Understanding of the Mechanisms of Maintaining Genomic Integrity for Therapeutic Purposes*. *Int J Mol Sci*, 2018. **19**(4).

45. Soule, H.D., et al., *Isolation and characterization of a spontaneously immortalized human breast epithelial cell line, MCF-10*. *Cancer Res*, 1990. **50**(18): p. 6075-86.
46. Puleo, J. and K. Polyak, *The MCF10 Model of Breast Tumor Progression*. *Cancer Res*, 2021. **81**(16): p. 4183-4185.
47. Petersen, O.W., et al., *Interaction with basement membrane serves to rapidly distinguish growth and differentiation pattern of normal and malignant human breast epithelial cells*. *Proc Natl Acad Sci U S A*, 1992. **89**(19): p. 9064-8.
48. Debnath, J., S.K. Muthuswamy, and J.S. Brugge, *Morphogenesis and oncogenesis of MCF-10A mammary epithelial acini grown in three-dimensional basement membrane cultures*. *Methods*, 2003. **30**(3): p. 256-68.
49. Muthuswamy, S.K., et al., *ErbB2, but not ErbB1, reinitiates proliferation and induces luminal repopulation in epithelial acini*. *Nat Cell Biol*, 2001. **3**(9): p. 785-92.
50. Mills, K.R., et al., *Tumor necrosis factor-related apoptosis-inducing ligand (TRAIL) is required for induction of autophagy during lumen formation in vitro*. *Proc Natl Acad Sci U S A*, 2004. **101**(10): p. 3438-43.
51. Zigrossi, A., et al., *SELENOF is a new tumor suppressor in breast cancer*. *Oncogene*, 2022.
52. Hanahan, D. and R.A. Weinberg, *Hallmarks of cancer: the next generation*. *Cell*, 2011. **144**(5): p. 646-74.
53. Kasaikina, M.V., et al., *Roles of the 15-kDa selenoprotein (Sep15) in redox homeostasis and cataract development revealed by the analysis of Sep 15 knockout mice*. *J Biol Chem*, 2011. **286**(38): p. 33203-12.
54. Sabry, A.O. and B.C. Patel, *Papilloma*, in *StatPearls*. 2023: Treasure Island (FL).
55. Gattelli, A., et al., *Progression of pregnancy-dependent mouse mammary tumors after long dormancy periods. Involvement of Wnt pathway activation*. *Cancer Res*, 2004. **64**(15): p. 5193-9.

56. Wellberg, E.A., et al., *Preventing ovariectomy-induced weight gain decreases tumor burden in rodent models of obesity and postmenopausal breast cancer*. *Breast Cancer Res*, 2022. **24**(1): p. 42.
57. Klintman, M., et al., *Postmenopausal overweight and breast cancer risk; results from the KARMA cohort*. *Breast Cancer Res Treat*, 2022. **196**(1): p. 185-196.
58. Lee, G.Y., et al., *Three-dimensional culture models of normal and malignant breast epithelial cells*. *Nat Methods*, 2007. **4**(4): p. 359-65.

## VITA

The author, Brenna, was born in Kirkland, Washington on February 28, 1995 to Kay Garbarino-Flowers and Steve Flowers. She attended Western Washington University in Bellingham, Washington where she earned a Bachelor's of Science (double major) in Kinesiology and Cellular and Molecular Biology in June 2019. After graduation, Brenna worked at CellNetix pathology lab and Adaptive Biotechnologies before she matriculated into the Loyola University Chicago Stritch School of Medicine Master Program, and began her graduate education in the Cellular and Molecular Oncology Program under the mentorship of Dr. Kastrati.

Brenna's thesis work on how the loss of SELENOF in combination with a Western Diet affects DMBA-induced tumorigenesis was supported by a Justice, Equity, Diversity, and Inclusion (JEDI) Focused Research Award from Loyola University Chicago. After completion of her graduate studies, Brenna will pursue a PhD in Loyola University Chicago's Integrated Program in Biomedical Sciences.



